

# PAMAM Dendrimers as Nanoscale Oral Drug Delivery Systems

Kelly M. Kitchens and Hamidreza Ghandehari

## Introduction

The application of nanotechnology to the diagnosis and treatment of diseases has coined the term *nanomedicine*. Nanometer-scale biomaterials have their role in nanomedicine since their nanoscopic size allows interaction with cellular membranes, subcellular organelles, passage through the microvasculature, and may reduce immunogenicity by avoiding reticuloendothelial uptake. Such features are desirable for nanomaterials to enhance the residence of poorly bioavailable drugs in the systemic circulation. Nanomaterials used as drug delivery systems, also termed nanocarriers, should be freely permeable to tumor vasculature since the endothelial pores range from 100 to 1000 nm (Hobbs et al., 1998). On the other hand, several moieties can be incorporated in these nanocarriers to enhance the delivery of bioactive and diagnostic agents. These include imaging agents for detection of the nanocarriers in the body, targeting ligands to direct the carrier to the site of action, enhanced cell permeation and intracellular trafficking with cell-penetrating moieties, as well as biodegradable linkers for drug release (Torchilin, 2006). Some examples of nanocarriers used for drug delivery applications include liposomes, micelles, polymers, and nanoemulsions, which have demonstrated the ability to serve as “multi-functional nanocarriers” (Torchilin, 2006). Water-soluble polymers have been used as targeted drug delivery systems since they can be designed to conjugate multiple drug compounds as well as targeting moieties. This results in alteration of a drug’s pharmacokinetic profile and therapeutic index by changing drug solubility, toxicity, biodistribution, and intracellular trafficking compared to free drug (Duncan & Spreafico, 1994; Luo & Prestwich, 2002; Tomlinson et al., 2003). The major drawback of such systems is their large size, which limits their administration primarily to parenteral routes that are invasive and require frequent physician visits.

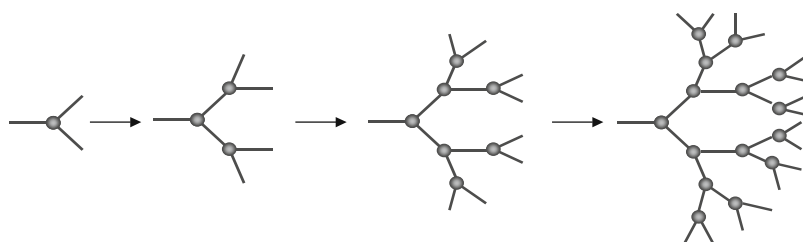
Oral drug administration offers high patient compliance due to the ease of administration, lack of discomfort and pain associated with injections, and lower cost. Yet a major limitation of polymers in oral drug delivery is their limited transport across the intestinal epithelium due to their large size relative to the tight, epithelial barrier of the gastrointestinal (GI) tract.

Furthermore, the acidic environment of the stomach along with various enzymes of the GI tract can affect the stability of polymeric drug delivery systems. In order to develop orally bioavailable polymers, it is essential to investigate their stability in the GI tract, interaction with the epithelial barrier of the gut, transepithelial transport and subcellular trafficking, systemic distribution, extravasation into the target tissue(s), and elimination from the body.

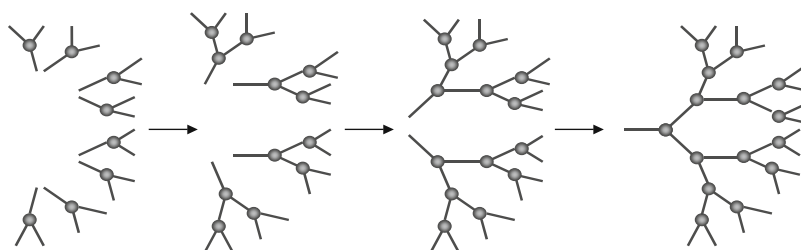
One class of polymers that have demonstrated potential use as oral drug delivery carriers are poly(amidoamine) (PAMAM) dendrimers (D'Emanuele & Attwood, 2005; Duncan & Izzo, 2005; Kitchens et al., 2005; Svenson & Tomalia, 2005). Recent studies have demonstrated that PAMAM dendrimers of certain generations and surface charge can permeate the epithelial barrier of the gut, suggesting their potential as oral drug delivery carriers (Jevprasesphant et al., 2003a; Kitchens et al., 2005, 2006; Wiwattanapatapee et al., 2000). PAMAM-drug conjugates have also shown the potential to bypass intestinal epithelial efflux pumps (D'Emanuele et al., 2004). The toxicity and biocompatibility of these systems is dependent on size, surface charge, and concentration (Duncan & Izzo, 2005; El-Sayed et al., 2002, 2003b; Jevprasesphant et al., 2003b; Kitchens et al., 2006), which can be modulated by surface modification, particularly of the positively charged primary amine groups (Jevprasesphant et al., 2003a,b; Kolhatkar et al., 2007; Roberts, 1996). Initial studies indirectly suggested that the transepithelial transport of PAMAM dendrimers is due to a combination of para- and transcellular pathways (El-Sayed et al., 2003b; Jevprasesphant et al., 2004). More recent studies have provided visual evidence that indeed PAMAM dendrimers open tight junctions, and endocytosis mechanisms contribute to their internalization and intracellular trafficking (Kitchens et al., 2007). These studies have set the stage for the use of PAMAM dendrimers as orally bioavailable nanocarriers. In this chapter a brief overview of the synthesis and characterization of dendrimers will be described, followed by a general account of their biocompatibility and applications in the delivery of bioactive and diagnostic agents. The main focus will be on the use of PAMAM dendrimers as oral drug carriers.

## Synthesis

Dendrimers involve the assembly of *dendrons* (Greek for “tree”) to form a *dendrimer* (Tomalia, 1993). Dendrimer synthesis involves the use of typical organic monomers to produce macromolecules with polydispersities of around  $\sim 1.0005$ – $1.10$  (Esfand & Tomalia, 2001; Tomalia, 2004). Two general synthetic methods have been used to produce dendrimers: the *divergent* and *convergent* methods (Scheme 14.1). The *divergent* method was pioneered by Tomalia and involves outward branching from an initiator core around which the branches of the dendrimer originates (Tomalia, 2004). The *convergent* method was introduced by Hawker and Fréchet, and involves inward growth from what will become the dendrimer surface to the inner core by the formation of individual dendrons (Hawker & Fréchet, 1990). Although these two strategies are traditionally used and have resulted in the production of several hundred dendrimer families (Svenson & Tomalia,



Divergent Synthesis



Convergent Synthesis

Scheme 14.1 Convergent and divergent synthesis of dendrimers.

2005), the synthetic approaches pose some challenges toward the commercialization of large quantities of dendrimer structures. Excess monomers and extensive purification techniques are required for the *divergent* process, while the *convergent* method is limited to the synthesis of lower generation (G) dendrimers due to steric hindrance that occurs from attaching outer dendrons toward the inner core (Svenson & Tomalia, 2005). To address these challenges, two alternative synthetic strategies have recently been introduced. One such method termed *lego chemistry* involves the synthesis of phosphorous-based dendrimers using functionalized cores and branched monomers, in which each generation is produced in a single-step reaction based on two types of alternating “layer blocks” (P(S)-OC<sub>6</sub>H<sub>4</sub>PPh<sub>2</sub>=NP(S) or P(S)NMeN=CHC<sub>6</sub>H<sub>4</sub>OP(S)) and the only byproducts are nitrogen and water (Brauge et al., 2001; Maraval et al., 2003). *Lego chemistry* produces phosphines, hydrazides, and aldehydes as end groups, which allow for further reactions to produce additional generations. For instance, this chemistry allows the number of surface groups to multiply from 48 phosphines of G4 to 250 aldehydes of G5 in one step (Maraval et al., 2003). *Click chemistry* is another alternative synthetic method that has been exploited for defined locations of dendritic block copolymers (Wu et al., 2004a, 2005). This chemistry involves Cu(I)-catalyzed formation of 1,2,3-triazole linkage to prepare azide-acetylene diblock dendrimers. The addition of mannose and coumarin units to the functional end groups of these dendrimers facilitates the dual function of biorecognition and detection, respectively (Wu et al., 2004a).

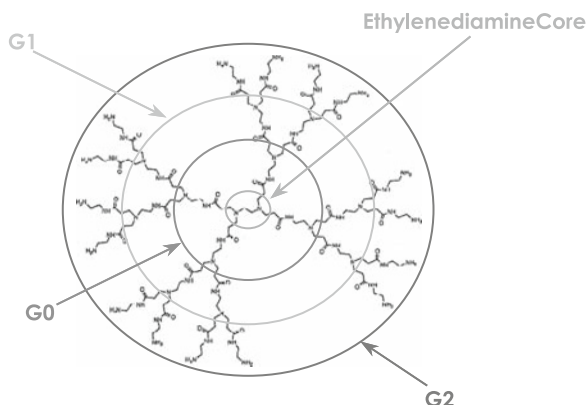
The selection of the initiator core, branching cells, and exterior functional groups can offer a countless variety of dendritic structures.

Poly(propyleneimine) (PPI) dendrimers are also commercially available with a diaminobutane (DAB) core. PPI dendrimers are synthesized using the divergent method via Michael addition of acrylonitrile to the primary amine groups, followed by hydrogenation of the nitrile groups to result in primary amine groups (Loup et al., 1999). Poly(ethyleneimine) (PEI) dendrimers are synthesized with an initiator core of ammonia, and alkylation of diethylenetriamine with aziridine produces the core shell tris-(2-aminoethyl)amine (Tomalia et al., 1990). Protected, first-generation PEI dendrimers are obtained through alkylation of the terminal amine groups with activated aziridines, followed by deprotection with acid hydrolysis (Tomalia et al., 1990). As the generation of PEI dendrimers increases, branching ideality decreases and branch defects are more likely due to de Gennes packing. PEI dendrimers have greater chemical and physical stability than poly(amidoamine) (PAMAM) dendrimers due to their shorter branch lengths (0.5 nm compared to 1 nm) (Tomalia et al., 1990). Starburst® dendrimers are commercially available as PAMAM or PPI with ethylenediamine or DAB cores, respectively, and are also available with cores diaminohexane, diaminododecane, and cystamine. The surface groups of Starburst® dendrimers include amino, sodium carboxylate, succinamic acid, tris-(hydroxymethyl) amidomethane, and poly(ethylene glycol) (PEG). Dendrimers typically used in biological applications include polyesters (Grinstaff, 2002), polypeptides (Sadler & Tam, 2002), and glycodendrimers (Turnbull & Stoddart, 2002). Table 14.1 gives an

**Table 14.1** Examples of types of dendrimers used for biomedical applications.

Dendrimer structure	Applications	References
PAMAM	Targeted delivery of paclitaxel in KB epidermoid carcinoma	Majoros et al., 2006
	Carrier for cisplatin in solid tumors	Malik et al., 1999
	Dendrimer-based Gd(III) chelates for MRI	Kobayashi and Brechbiel, 2005
	Cardiac diagnostic marker, e.g., Stratus® CS manufactured by Dade Behring	Halford, 2005
	Permeation enhancer for propranolol in Caco-2 epithelial cells	D'Emanuele et al., 2004
	Carrier for ibuprofen in A549 lung epithelial cells	Kolhe et al., 2006
PPI	Gene transfection agent for nucleic acids, e.g., Superfect® manufactured by Qiagen	Dufes et al., 2005b
	Preventing scar tissue formation	Shaunak et al., 2004
	Vector for TNF- $\alpha$ gene therapy of A431 epidermoid carcinoma, C33a cervix carcinoma, and LS174T colorectal adenocarcinoma	Dufes et al., 2005a
	Dendrimer-based Gd (III) chelates for MRI	Kobayashi and Brechbiel, 2005
Polypeptide	Gene transfection agent for nucleic acids	Dufes et al., 2005b
	Carrier of ara-C prodrugs for tumor inhibition	Choe et al., 2002
Polyester	Potential targeted drug delivery carrier to tumor cells	Tansey et al., 2004
	Carrier for anti-cancer agent doxorubicin in murine melanoma cell line; improved doxorubicin biodistribution in vivo	Padilla De Jesus et al., 2002
	Adhesive to repair corneal lacerations	Velazquez et al., 2004

Scheme 14.2 Schematics of amine terminated PAMAM dendrimers: G denotes generation. Adapted from Tajarobi et al. (2001) (with permission from Elsevier).



overview of some dendrimer structures that have been employed in biomedical applications.

The focus of this article is on PAMAM dendrimers, which are the first dendrimer family to be completely synthesized, characterized, and commercialized (Tomalia, 2004). PAMAM dendrimers are synthesized using the *divergent* method, and dendrimer growth occurs in a radial fashion around a nucleophilic core (Scheme 14.2). The surface groups increase exponentially and the molecular mass of dendrimers increases almost twofold due to the inner core ( $N_c$ ) and branch cell ( $N_b$ ) multiplicity (Tomalia, 2004). PAMAM dendrimers are generally constructed with an initiator core (e.g., ethylene diamine or ammonia) where branching occurs via Michael addition of the amines with methyl acrylate to produce a half-generation (e.g., G0.5). This is followed by amidation of the ester groups with excess ethylene diamine to result in a full generation dendrimer with primary amine surface groups (e.g., G1) (Tomalia, 1993, 2004).

The molecular size of PAMAM dendrimers increases by approximately 1 nm with each generation, with sizes ranging from 1 to 15 nm (Esfand & Tomalia, 2001; Tomalia, 2004). The polydispersity values of PAMAM dendrimers range from  $\sim 1.000002$  to 1.005 verified by gel electrophoresis and matrix-assisted laser desorption ionization time of flight (MALDI-TOF) mass spectrometry (Brothers II et al., 1998; Esfand & Tomalia, 2001).

## Characterization

A major advantage of dendrimers over traditional polymers is the precise control over their architecture that results in monodispersed structures. This is a significant feature when considering the transport and biodistribution of nanostructures for drug delivery applications. Thus, it is crucial to employ analytical techniques to characterize and verify the structure of dendrimers. The monodispersity of dendrimers has typically been verified using size-exclusion chromatography, gel electrophoresis, mass spectrometry, and transmission electron microscopy (TEM) (Tomalia, 2004). Size-exclusion chromatography separates molecules on the basis of

molecular size, where large molecular weight molecules elute from a chromatography column earlier than small molecular weight molecules, and this technique is typically used to monitor dendrimer size, molecular mass, and polydispersity (Caminade et al., 2005). Polydispersities of 1.01–1.08 for G0–G9 have been obtained by size-exclusion chromatography (Tomalia et al., 1990), and when coupled with laser light scattering techniques it is used to determine the hydrodynamic radii of dendrimers (Caminade et al., 2005; Tomalia et al., 1990). Polyacrylamide gel electrophoresis (PAGE) analyses have shown that the mobility of PAMAM-succinamic dendrimers slows as the generation increases from 2 to 7, while capillary zone electrophoresis separated dendrimers based on their charge/mass ratio (Sedlakova et al., 2006; Shi et al., 2005). Comparative studies using native PAGE and sodium dodecyl sulfate (SDS)-PAGE analyses of PAMAM dendrimers revealed smaller G2 dendrimer migrated further than the larger G4 dendrimer (Kolhatkar et al., submitted). Dendrimer migration retarded with a decrease in the number of positively charged groups in PAGE analysis but dendrimers migrated further when the surface groups were completely acetylated and subjected to SDS-PAGE analysis (Kolhatkar et al., 2007). The difference in observations occurred because native PAGE separates compounds on the basis of charge and molecular weight, whereas SDS-PAGE separation is achieved on the basis of molecular weight only.

Mass spectrometry has revealed that convergent dendrimer synthesis produces the most monodisperse dendrimers since each growth step involves purification, which eliminates dendrimer imperfections such as branch defects and failed amidoamine couplings (Tomalia, 2004). Lower generation dendrimers (G0–G5) that are synthesized via the divergent method are also quite monodisperse as evidenced by mass spectrometry measurements that are consistent with the predicted mass values. The predicted mass values of higher generation dendrimers tend to deviate from theoretical values due to de Gennes packing, although their polydispersity remains very narrow (i.e., 1.05) (Tomalia, 2004; Tomalia et al., 1990). The characterization of dendrimers with mass of less than 3000 Da is limited to chemical ionization and fast atom bombardment mass spectrometry techniques. Higher generation dendrimers have been characterized with electro-spray ionization (ESI) and Fourier transform ion cyclotron resonance (FT-ICR) (Felder et al., 2005; Hummelen et al., 1997) as well as MALDI-TOF (Caminade et al., 2005). TEM has allowed the visualization of PAMAM dendrimer molecules (G5–G10) to compare their molecular sizes (Jackson et al., 1998). Intrinsic viscosity measurements also offer insight into the dimensional properties of dendrimers (Tomalia et al., 1990). Dendrimer volume grows faster than molecular weight with an increase in earlier generations, and vice versa for generations beyond the intrinsic viscosity maxima (Caminade et al., 2005).

Nuclear magnetic resonance (NMR) spectroscopy has been employed to verify the structure of dendrimers.  $^{13}\text{C}$ -NMR has proven an effective method for confirming branching ideality, due to distinct resonances for ideal dendrimer branching versus incomplete acrylate alkylations (Tomalia et al., 1990).  $^1\text{H}$ -,  $^{13}\text{C}$ -, and  $^{15}\text{N}$ -NMR are often used to

characterize the interior and end groups of organic dendrimers due to the chemical changes that occur with each branching step (Caminade et al., 2005; Tomalia et al., 1990), and particularly to confirm the functionalization of dendrimer surface groups (Hong et al., 2004a; Jevprasesphant et al., 2003a; Kolhatkar et al., 2007; Sanchez-Sancho et al., 2002), the conjugation of therapeutically active molecules (Khandare et al., 2005; Kolhe et al., 2004; Tang et al., 2006), imaging agents (Fu et al., 2006), and targeting moieties (Majoros et al., 2006). Two- and three-dimensional NMR techniques ( $^1\text{H}$ -,  $^{13}\text{C}$ -) have also been used to characterize dendritic structures such as polyaryl (Rajca, 1991) and poly(propyleneimine) (PPI) dendrimers (Boas et al., 2001; Chai et al., 2001) when complex pulse sequences are required for appropriate signal assignment (Caminade et al., 2005). For “inorganic” dendrimers, additional NMR techniques such as  $^{31}\text{P}$ -NMR for phosphorous dendrimers (Launay et al., 1995),  $^{29}\text{Si}$ -NMR for silicon-based dendrimers (Chai et al., 1999), and  $^{19}\text{F}$ -NMR for fluorinated end groups (Sakamoto et al., 2000) are used. Infra-red (IR) spectroscopy is also used to analyze chemical transformations during dendrimer synthesis and modifications (Tomalia et al., 1990), such as the synthesis of poly(aromatic amide) dendrimers using coupling steps via the convergent process (Aulenta et al., 2005), formation of cross-linked hydrogels composed of poly(vinyl alcohol) (PVA) and G6 PAMAM-NH<sub>2</sub> dendrimers through hydrogen bonding (Wu et al., 2004b), and the complexation of ibuprofen to PAMAM-NH<sub>2</sub> dendrimers (Kolhe et al., 2003).

Small-angle X-ray scattering (SAXS) techniques can be used to determine the size, shape, and internal structure of monodispersed polymers based on the intensity distribution of scattered particles as a function of scattering angles from an irradiated X-ray beam (Trehwella et al., 1998). The internal structure of PAMAM dendrimers, G0–G8, has been determined using SAXS measurements (Rathgeber et al., 2004). SAXS measurements of G3 PAMAM dendrimers have revealed structures that resemble star-like molecules, whereas larger generations, 9 and 10, had scattering features that were consistent with hard, sphere-like molecules (Prosa et al., 2001). Small-angle neutron scattering (SANS) techniques also give insight into the molecular structure of dendrimers, as well as inter- and intra-molecular associations. SANS measurements are based on the difference in scattering lengths between hydrogenous monomer units of structures in deuterated solvent (Wignall & Melnichenko, 2005). For instance, the scattering profiles of carboxyl-terminated dendrimers in solution was concentration dependent as indicated by interdendrimer interactions (Huang et al., 2005). Furthermore, SANS measurements have demonstrated silbenoid dendrimers exist as thick (1.8 nm), circular disks in deuterated toluene, whereas SAXS measurements only provided insight that these dendrimers exist as circular disks (Rosenfeldt et al., 2006). The molecular weight of G5 dendrimers in deuterated dimethylacetamide has been measured using SANS techniques (Potschke et al., 1999). In these studies, SANS measurements yield the contrast  $\rho - \rho_m$ , where  $\rho$  is the average scattering length density of the dissolved dendrimer and  $\rho_m$  is the scattering length density of the solvent, which allows molecular weight determination of the dendrimer.

## Biocompatibility

The toxicity and biocompatibility of dendrimers must be considered for biomedical applications. One of the earlier accounts of testing dendrimer biocompatibility demonstrated a generation-dependent toxicity of PAMAM-NH<sub>2</sub> dendrimers (G3, G5, and G7) *in vitro* and *in vivo* (Roberts et al., 1996). Immunogenicity was not observed with these dendrimers. G3 dendrimers had the greatest accumulation in the kidneys of Swiss-Webster mice (15% ID/g after 48 hours), while G5 and G7 dendrimers had peak levels in the pancreas (32% ID/g at 24 hours, 20% ID/g at 2 hours, respectively) (Roberts et al., 1996). Additional studies investigated the toxicity and biodistribution of <sup>125</sup>I-labeled PAMAM dendrimers administered intravenously (*i.v.*) and intraperitoneally (*i.p.*) in male Wistar rats (Malik et al., 2000). Dendrimers with cationic amino groups (G1–G4) were generally hemolytic and displayed generation-dependent effect on cytotoxicity, whereas anionic carboxylate-terminated and carbosilane dendrimers were neither hemolytic nor cytotoxic after 1 hour. Yet the hemolytic activity of anionic and carbosilane dendrimers increased after 24 hours, and it was proposed the hemolytic behavior was caused by hydrophobic membrane interaction with the aromatic core of carbosilane dendrimers. Additionally, cationic dendrimers (G3, G4) were rapidly cleared from the circulation after *i.v.* and *i.p.* administration. In contrast anionic dendrimers had greater circulation times (15–40% recovered in blood after 1 hour) in a generation-dependent manner with appreciable liver accumulation (25–70% of recovered dose). To investigate the potential of PAMAM dendrimers as oral delivery systems, the glucose active transport assay was used to assess dendrimer toxicity, in which anionic dendrimers were able to transport glucose up to 100 µg/ml, while cationic G4 caused cytotoxicity at this concentration (Wiwattanapatapee et al., 2000). These initial studies suggested dendrimer architecture can be tailored based on size and surface chemistry to avoid toxicity, enhance transport across epithelial barriers, and/or prolong systemic circulation.

Cationic macromolecules have a favorable interaction with negatively charged cell membranes which leads to their enhanced uptake and increased toxicity caused by an osmotic imbalance (Karoonthaisiri et al., 2003). Several studies have reported hole formation and lipid bilayer disruption caused by cationic dendrimers (Hong et al., 2004b, 2006; Mecke et al., 2005, 2004). Atomic force and fluorescence microscopy studies demonstrated cationic G7 dendrimers (10–100 nM) formed holes in 1,2-dimyristoyl-*sn*-glycero-3-phosphocholine (DMPC) lipid bilayers of 15–40 nm in size. G3 and G5 dendrimers did not form holes in these studies although G5 expanded holes at existing defects and were non-toxic up to 500 nM (Hong et al., 2004b, 2006; Mecke et al., 2005, 2004). Studies demonstrated that electrostatic interaction between the positively charged dendrimers and negatively charged lipid bilayers causes internalization of molecules (Hong et al., 2004b), and the lack of electrostatic interactions reduces the ability of dendrimers to disrupt the cell membranes (Mecke et al., 2004). These studies further suggest cytotoxicity is more likely to occur with cationic dendrimers of higher generations and



donor concentration. This is also demonstrated by TEM observations, which show that the application of large, cationic dendrimers to Caco-2 cells resulted in the loss of microvilli unlike anionic dendrimers (Figure 14.1A) (Kitchens et al., 2007). Further loss of microvilli occurred with an increase in G4NH<sub>2</sub> concentration (Figure 14.1B). Among a series of dendrimers with surface groups of amine, guanidine, carboxylate, sulfonate, phosphonate, and PEGylated, the cationic dendrimers were more cytotoxic based on the 3-(4,5-dimethylthiazole-2-yl)-2,5-diphenyltetrazolium bromide (MTT) assay compared with anionic and PEGylated dendrimers (Chen et al., 2004). Several studies have demonstrated the reduction of cationic dendrimer cytotoxicity when the surface groups were modified with hydrophobic moieties or PEG chains (Jevprasesphant et al., 2003a,b; Kitchens et al., 2006; Kolhatkar et al., 2007). It should be noted that dendrimer toxicity is not solely based on its surface chemistry. As previously mentioned, poly(ethylene oxide) (PEO)-modified carbosilane dendrimers did cause

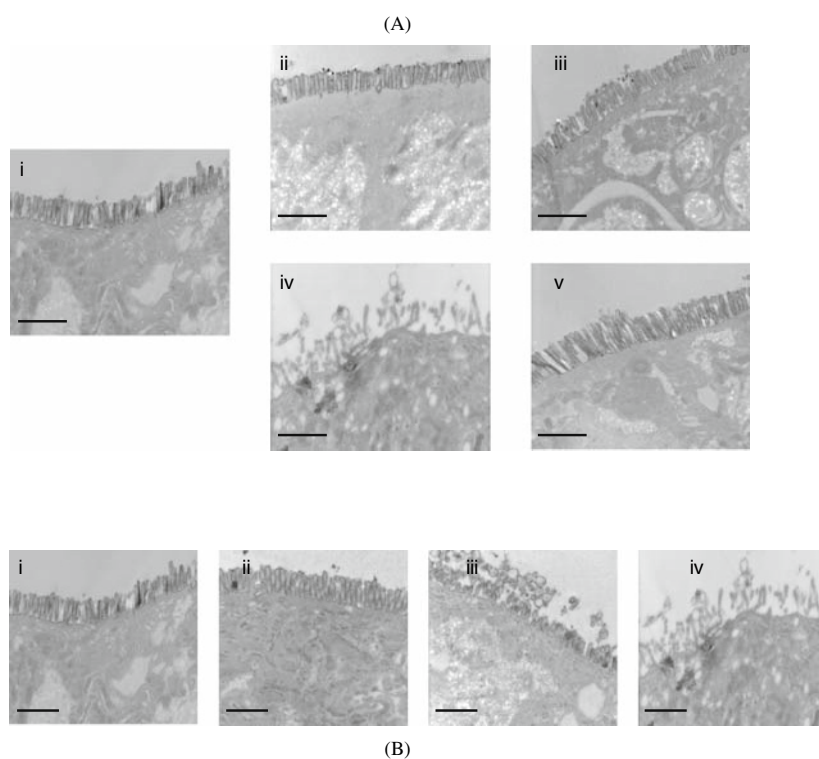


**Figure 14.1** (A) Transmission electron microscopy (TEM) images of Caco-2 cell monolayers after treatment with PAMAM dendrimers (1 mM) for 2 hours: (i) control cells; (ii) G2NH<sub>2</sub>; (iii) G1.5COOH; (iv) G4NH<sub>2</sub>; (v) G3.5COOH. The images display a generation-dependent effect of PAMAM dendrimers on Caco-2 microvilli (magnification = 12,500 $\times$ ). (B) TEM images of Caco-2 cell monolayers after treatment with G4NH<sub>2</sub> dendrimers for 2 hours: (i) control cells; (ii) 0.01 mM G4NH<sub>2</sub>; (iii) 0.1 mM G4NH<sub>2</sub>; (iv) 1.0 mM G4NH<sub>2</sub>. The images display a concentration-dependent effect of G4NH<sub>2</sub> on Caco-2 microvilli (magnification = 12,500 $\times$ ). Scale bars = 1  $\mu$ m. Adapted from Kitchens et al. (2007) (with permission from ACS Publications).

hemolysis *in vivo* due to interactions between the aromatic core and the hydrophobic cell membranes (Malik et al., 2000). Furthermore, low generation dendrimers possess a more open molecular structure, which makes a possibly toxic core and surface groups more accessible to interact with the cell membranes (Duncan & Izzo, 2005). Along with molecular weight and surface charge density, the extent of polycation cytotoxicity can also depend on molecular conformation. For instance, PAMAM dendrimers have a compact, spherical structure in solution and were found to be less cytotoxic than linear polycations (Fischer et al., 2003).

Several studies have been conducted on the toxicity of dendrimers *in vivo* to date. For instance, the deaths of three mice were reported after administration of G7 dendrimers over a 2-hour period (Roberts et al., 1996). No toxicity or mortality was observed among C3H mice when single doses of PEGylated melamine were administered as 2.56 g/kg *i.p.* or 1.28 g/kg *i.v.* over 24 and 48 hours, respectively (Chen et al., 2004). Polyester-based dendrimers with hydroxyl or methoxy surface groups caused some inhibition of cell growth *in vitro*, but did not induce cell death up to 40 mg/ml (Padilla De Jesus et al., 2002). Mortality was only observed in one animal after 24 hours when these dendrimers were administered as a single dose (1.3 g/kg) (Padilla De Jesus et al., 2002). Additionally, the efficacy of dendrimer-based antiviral topical microbicides was demonstrated against herpes simplex virus type 2 (HSV-2) in female Swiss-Webster mice. Bourne et al. (2000) have reported the synthesis of PAMAM (BRI-6039) and polylysine dendrimers (BRI-2999 and BRI-6741) by the Biomolecular Research Institute (BRI, Parkville, Victoria, Australia) by the addition of polylysine repeat units to a benzhydrylamine core, with capping layers of naphthyl disodium disulfonate (BRI-2999) and phenyl disodium dicarboxylate (BRI-6741). Intravaginal application of BRI-6039, BRI-2999, and BRI-6741 significantly reduced the incidence of HSV-2 compared to control treatments, but only BRI-2999 dendrimers prevented infection when administered immediately and 30 minutes before intravaginal challenge. This research has led to the development of VivaGel<sup>TM</sup>, a topical microbicide for the prevention of HIV and other sexually transmitted diseases (Jiang et al., 2005) by Starpharma Ltd. (Melbourne, Victoria, Australia). Phase I clinical studies investigated the safety of VivaGel<sup>TM</sup> in a double-blinded study, and no irritation or inflammation was observed for the healthy women that received intravaginal doses of the gel (Svenson & Tomalia, 2005).

## Dendrimers for Delivery of Bioactive Agents

Bioactive agents can be complexed with dendrimers by electrostatic interactions, chemically conjugated to the surface terminal groups, or incorporated within the dendritic box. Numerous groups have studied the use of dendrimers for the delivery of therapeutic and diagnostic agents. Comprehensive review of these reports are beyond the scope of this chapter and the reader is referred elsewhere (Cloninger, 2002; D'Emanuele & Attwood, 2005; Dufes et al., 2005b; Duncan & Izzo, 2005; Kobayashi & Brechbiel, 2005; Lee et al., 2005; Liu & Frechet, 1999; Patri et al., 2005; Svenson &

Tomalia, 2005). A few examples for delivery of nucleic acids, imaging agents, and small molecular weight drugs are discussed below.

Amine-terminated dendrimers such as PAMAM or PPI have been used as gene transfection agents (Dufes et al., 2005b). Haensler and Szoka (1993) were the first to demonstrate that PAMAM dendrimers efficiently express reporter genes in a suspension of mammalian cells. Maximal luciferase expression was achieved with G6 and a dendrimer to DNA charge ratio of 6:1. PAMAM dendrimer/DNA complexes showed lower toxicities than polylysine and greater transfection efficiency (Behr, 1994; Haensler & Szoka, 1993). It was thought that the enhanced efficiency of dendrimers occurred since they did not require lysosomotropic agents to escape the endosomes, but dendrimers have the ability to escape endosomes via the proposed “proton sponge” effect (Behr, 1994; Haensler & Szoka, 1993). This theory postulates that lysosomotropic activity occurs through protonation of the tertiary amine groups in PAMAM dendrimers, resulting in osmotic swelling of the endosomal compartments, thus leading to enhanced DNA delivery to the cytoplasm (Haensler & Szoka, 1993). In general, dendrimers enhance DNA expression by condensing the nucleic acids and acting as an endosomal pH buffer (Hughes et al., 1996). Interestingly “fractured” dendrimers were more effective transfection agents possibly due to their increased flexibility allowing nucleic acid release (Tang et al., 1996).

To increase circulation time and decrease toxicity, PAMAM-PEG-PAMAM triblock copolymers were synthesized which formed stable water-soluble complexes with high transfection efficiency in 293 cells (Kim et al., 2004). Although dendrimers promise to be effective delivery systems for gene therapy, issues such as toxicity and efficacy remain a concern for in vivo and clinical applications. Recent reports have demonstrated PPI dendrimers (G2, G4 and G5) display low cytotoxicity in several human cell lines when interior and exterior amines were modified with methyl iodide/chloride and carboxylic acid derivatives, respectively (Tack et al., 2006). These modified PPI dendrimers also enhanced the transfection efficiency of DNazyme in ovarian cells, while dendrimer-DNazyme complexes were localized in tumor nuclei following intravenous injection in Nude mice (Tack et al., 2006). These findings suggest the efficiency and safety of PPI dendrimers for gene therapy. Additionally, lipidic poly (lysine) dendrimers enhanced the intracellular delivery of recombinant firefly luciferase and a c-myc monoclonal antibody compared in various cell lines, which demonstrates the potential application of these peptidic dendrimers in protein therapeutics (Bayele et al., 2006).

Additional studies have investigated dendrimers for delivery of oligonucleotides. PAMAM dendrimer G5 was used to deliver antisense oligodeoxynucleotides and reduce chloramphenicol acetyl-transferase (CAT) expression in CHO cell lines by approximately 38% (Hughes et al., 1996). PAMAM:oligonucleotide complexes increased the intracellular uptake of oligonucleotides in astrocytoma cells 3- to 4-fold with 1:1 dendrimer:oligonucleotides and 50-fold for 20:1 complexes, as well as increased delivery to the nucleus (Bielinska et al., 1996; DeLong et al., 1997). Confocal microscopy and cell fractionation studies revealed oligonucleotide-dendrimer complexes are localized in the nucleus of HeLa cells, which suggests

dendrimers are capable of delivering oligonucleotides to nuclei where they exert their pharmacological actions and the complex remains intact unlike other cationic delivery agents that are typically degraded in the endosomes (Yoo & Juliano, 2000). Further studies revealed that while PAMAM dendrimers are effective in antisense oligonucleotide delivery, they are less effective in siRNA oligonucleotide delivery most likely due to incomplete release of siRNA from dendrimer (Kang et al., 2005). Furthermore, antisense and siRNA oligonucleotides delivered by PAMAM and TAT-PAMAM conjugates partially inhibited P-glycoprotein (P-gp) expression in NIH 3T3 multi-drug resistant cells at low concentrations, and greater inhibition was observed with higher dendrimer concentrations, yet greater toxicity was observed at these concentration levels (Kang et al., 2005). Although these studies demonstrate dendrimers are less effective than cationic lipid delivery agents, they are probably more suitable carriers for oligonucleotides since they are smaller than cationic lipid particles and would be less susceptible to rapid clearance (DeLong et al., 1997; Juliano, 2006).

Dendrimer-based contrast agents for magnetic resonance imaging (MRI) have allowed for enhanced MR images *in vivo* attributed to longer blood circulation, greater extravasation, and improved excretion compared to other macromolecular contrast agents (Kobayashi & Brechbiel, 2005). The free amines of PAMAM dendrimers have been conjugated to gadolinium (Gd) chelates, which exhibited greater molecular relaxivities than metal-chelate conjugates of other macromolecules including serum albumin, poly(lysine), and dextran. These dendrimer-based agents displayed longer enhancement half-lives than Gd(III)-diethylenetriaminepentaacetic acid (Gd(III)-DTPA) (Wiener et al., 1994). These earlier studies demonstrated the potential use of dendrimers as MRI contrast agents. PAMAM dendrimers (G6) with either ammonia (G6A) or ethylene diamine cores (G6E) were compared in terms of their blood retention, biodistribution, and renal excretion. <sup>153</sup>Gd-labeled G6E2-(*p*-isothiocyanatobenzyl)-6-methyl-diethylenetriaminepentaacetic acid (1B4M) conjugates had longer retention in the circulation due to more exterior amine groups available in G6E (256 amine groups) than G6A (192 amine groups) to react with Gd atoms. G6A-1B4M-Gd(III) had brighter kidney images, as well as faster clearance and higher renal accumulation, than G6E-1B4M-Gd(III) due to enhanced glomerular filtration (Kobayashi et al., 2001b). The conjugation of two PEG molecules to G4-1B4M-Gd resulted in prolonged retention in the circulation, increased excretion, and decreased accumulation in the liver and kidneys, compared to PEG(1)-G4-1B4M-Gd and G4-1B4M-Gd (Kobayashi et al., 2001a). DAB-based contrast agents displayed greater relaxivity than ammonia core PAMAM-based agents of similar size (G2) (Wang et al., 2003). Higher generation PPI contrast agents (G3 and G5) had prolonged blood signal enhancement than smaller (G0 and G1) dendritic agents (Langereis et al., 2006) suggesting higher generation PPI-based contrast agents may be more suitable for MRI than PAMAM-based agents.

Previous reports demonstrated PAMAM G4-Gd complexes conjugated to folic acid were capable of imaging tumors that expressed the folate receptor (Konda et al., 2000) and that dendrimer-folate conjugates do target and internalize within folate-expressing cells (Quintana et al.,

2002). Other applications of dendrimer-based diagnostics have included DNA-assembled dendrimers to target cancer cells (Choi et al., 2005). In these systems, oligonucleotides were used to self-assemble to PAMAM dendrimers (G5 or G7), one conjugated to folic acid to target KB cancer cells that over-express the folate receptor, while the other dendrimer was conjugated to fluorescein isothiocyanate (FITC) as an imaging agent (Choi et al., 2005). Dendritic contrast agents were prepared by the synthesis of dendrimers with PEG cores and *tert*-butyloxycarbonyl-L-lysine-generated branching architecture to generate G3–G5, followed by the conjugation of a clinically used computed tomography (CT) contrast agent, iobitridol, to their lysine amino groups (Fu et al., 2006). These dendritic contrast agents are being explored for potential use in CT imaging due to their prolonged circulatory retention, and potential toxicity reduction of iodinated small molecules (Yordanov et al., 2002). Dendrimers have also been used in oxygen imaging diagnostics, in which metalloporphyrins were encapsulated in the cores of poly(glutamic acid), poly(aryl ether), and poly(ether amide) dendrimers to create water-soluble oxygen sensors (Dunphy et al., 2002). In these applications, the phosphorescence lifetime of the dendrimers is inversely proportional to oxygen concentration in tumors, which indicates if the tumor would respond to treatment (Ziemer et al., 2005).

Dendrimers have also been used for the delivery of small molecular weight drugs. When the anti-cancer drug cisplatin was encapsulated in PAMAM dendrimers with a payload of ~25%, lower toxicity, slower release, and increased accumulation in solid tumors were achieved compared to cisplatin alone (Malik et al., 1999). Other chemotherapeutic agents including doxorubicin and 5-fluorouracil have been conjugated to dendrimers, which allowed the release of these drugs *in vitro* (Ihre et al., 2002; Padilla De Jesus et al., 2002; Zhuo et al., 1999). Similarly, dendrimer-propranolol conjugates increased the permeability of propranolol, a P-gp substrate, through bypassing the P-gp system (D'Emanuele et al., 2004). Another group has investigated the effect of PAMAM dendrimers and Perstrop Polyol, a fifth generation hyperbranched poly ester with hydroxyl surface groups, on the cellular entry of ibuprofen (Kannan et al., 2004; Kolhe et al., 2004, 2003). Ibuprofen was successfully complexed to all the surface groups of PAMAM dendrimers G3 and G4, and some ibuprofen was encapsulated in PAMAM G4, while the hyperbranched polyol was able to incorporate some ibuprofen without complexation due to the lack of electrostatic interactions between hydroxyl surface groups and carboxyl groups of ibuprofen (Kolhe et al., 2003). The ibuprofen-PAMAM complexes maintained the anti-inflammatory effect of ibuprofen, and ibuprofen displayed greater suppression of COX-2 in the complexed form compared to pure ibuprofen. Additionally, hyperbranched polyol- and polyglycerol-ibuprofen conjugates showed increased inhibition of prostaglandin synthesis compared to ibuprofen (Kolhe et al., 2004), as did methylprednisolone conjugated to G4OH via a glutaric acid spacer (Khandare et al., 2005). These studies demonstrate that dendrimers can carry a high therapeutic payload, are capable of maintaining the pharmacological activity of drugs, and can improve drug release to the site of action compared to free drug. Dendrimers have also been applied as solubility enhancers for poorly soluble, hydrophobic drugs (Milhem

et al., 2000), and dendrimer solubility enhancement has proven to be a function of surface chemistry (Chauhan et al., 2003), generation where solubility increased with generation number (Namazi & Adeli, 2005), and core chemistry which affects dendrimer flexibility (Liu et al., 2000).

In summary, dendrimers clearly offer many advantages in the delivery of bioactive and diagnostic agents. Their potential as drug carriers arises from the large number of surface groups to immobilize drugs, enzymes, targeting moieties, or other bioactive and imaging agents. These macromolecules are capable of enhancing drug solubility, increasing drug circulation due to their nanoscopic size, and targeted delivery with the incorporation of specific ligands to the surface groups. Due to the need to develop orally bioavailable polymeric drug delivery systems and the potential use of dendrimers in drug delivery applications, it is highly desirable to develop dendrimer-based drug delivery systems that are orally bioavailable.

## **PAMAM Dendrimers as Potential Oral Drug Delivery Carriers**

### **Oral Absorption of Dendrimers**

The first reports to demonstrate the oral administration of a dendrimer structure involved a lipidic polylysine dendrimer in Sprague–Dawley rats (Florence et al., 2000; Sakthivel et al., 1999). A dendrimer molecule of mean diameter 2.5 nm was synthesized and radiolabeled with tritium. A rapid uptake of the dendrimer within the GI tract was observed since 2% of administered dose was recovered from the stomach after 3 hours and less than 1% after longer times. The amount of dendrimer recovered in additional GI organs increased from 3 to 6 hours (Sakthivel et al., 1999). For instance, rapid absorption of the dendrimer was observed as indicated by 15 and 5% recovery of administered dendrimer in the small and large intestines after 6 hours, respectively. Overall, at least 20% of administered dendrimer was recovered in the stomach, small and large intestines after 6 hours, yet only 1% was recovered in these organs after 24 hours (Florence et al., 2000; Sakthivel et al., 1999). Furthermore, the amount of administered dendrimer recovered in the liver, kidneys, spleen, and blood increased from 3 to 6 hours, and approximately 1.2 and 3% of administered dose was recovered in the liver and blood, respectively, after 6 hours, while less than 1% was recovered in the spleen and kidneys as well as in all organs after 24 hours. These studies demonstrated the rapid absorption of the dendrimer after 24 hours in the GI tract.

Additional studies focused on comparing the uptake and transport rates of the dendrimer (2.5 nm) and polystyrene latex nanoparticles ranging from 50 to 3000 nm in diameter (Florence et al., 2000). After 10 days 15% of dendrimer and 12% of 50-nm polystyrene particles were recovered from the small intestine, although the dendrimer had less cumulative uptake in the liver and spleen than 50-nm polystyrene particles. The cumulative uptake of dendrimers in the liver, spleen, kidneys, and blood was less than that of the 50-nm polystyrene particles, which could be

explained by the greater amount of dendrimers detected in the blood due to slower rates of perfusion. It was anticipated that the smaller dendrimer would have greater uptake than the 50-nm latex nanoparticles, since previous studies suggested gut-associated lymphoid tissue uptake is size dependent over a range of 50–3000 nm nanoparticles (Florence, 1997). Further studies investigated how dendrimer generation and GI fluid influence the formation of aggregates (Singh & Florence, 2005). These studies suggested increase in generation number results in an increase in the number of lipid chain groups, which led to dendrimer aggregation.

Variations in dendrimer concentration affected aggregate formation, in which increased concentration for lower generation dendrimers ( $C_4$  surface lipid chains) resulted in increased mean number diameter, whereas larger dendrimers ( $C_{10}$  and  $C_{12}$  surface lipid chain) had smaller diameters with an increase in dendrimer concentration. These observations indicated the dendrimers with shorter alkyl-chain surface groups had greater surface hydrophobic interactions that resulted in dendrimer aggregation. Finally, the stability of polylysine dendrimers was studied in GI fluid for 3 hours. The dendrimers were stable in intestinal fluid, however, the acidic environment of the stomach led to self-association of the dendrimer particles, which was evidenced by the increase in their hydrodynamic diameter (Singh & Florence, 2005). The smaller nanoparticles and lower generation dendrimers were more susceptible to aggregate formation due to their increased flexibility and thus accessibility to self-associate, and to possibly adsorb to the cell membrane. This may explain the lower uptake observed for 2.5-nm dendrimers compared to 50-nm polystyrene nanoparticles in the GI tract.

### Transepithelial Transport of Poly(amidoamine) Dendrimers

One of the first studies to demonstrate the ability of PAMAM dendrimers to cross the GI tract investigated their rate of uptake and transport using everted rat intestinal sacs as an *in vitro* model of the intestinal epithelial barrier (Wiwattanapatee et al., 2000). Cationic (G3 and G4) and anionic PAMAM dendrimers (G2.5, G3.5, and G5.5) were  $^{125}\text{I}$ -labeled, and the amounts recovered in the tissue and serosal fluid were measured as a function of time. A major finding from this study was that cationic PAMAM dendrimers showed greater tissue uptake (3.3–4.8  $\mu\text{L}/\text{mg}$  protein/h) than their serosal transfer rates (2.3–2.7  $\mu\text{L}/\text{mg}$  protein/h) at each time point, whereas anionic G2.5 and G3.5 showed greater serosal transfer rates (3.4–4.4  $\mu\text{L}/\text{mg}$  protein/h) than their tissue uptake (0.6–0.7  $\mu\text{L}/\text{mg}$  protein/h). Anionic G5.5 had greater tissue uptake (2.48  $\mu\text{L}/\text{mg}$  protein/h) than that of G2.5 and G3.5. The amount of G5.5 recovered in serosal fluid (65–70%) was less than that of G2.5 and G3.5 (80–85%). In summary, this study showed that cationic dendrimers had greater tissue association than anionic dendrimers of similar size, while anionic G5.5 had greater tissue accumulation than smaller G2.5 and G3.5.

The permeability of a series of cationic PAMAM-NH<sub>2</sub> dendrimers, G0–G4, was measured as a function of dendrimer generation and concentration across Madin–Darby Canine Kidney (MDCK) cells as model monolayers to assess their transepithelial transport (Tajarobi et al., 2001).

MDCK cells were used as a preliminary screening tool since drug permeability rates across MDCK cells is similar to Caco-2 cell permeability (Irvine et al., 1999). PAMAM dendrimers were fluorescently labeled with FITC, and the fluorescently labeled dendrimers were fractionated by size-exclusion chromatography techniques to ensure the permeability values were not attributed to small molecular weight fragments. The rank order of PAMAM permeability was  $G4 \gg G0 \approx G1 > G3 > G2$ , with apparent permeability ( $P_{app}$ ) values ranging from 0.076 to  $16.1 \times 10^6$  cm/s. These results demonstrated a clear relationship between dendrimer size and their transport. PAMAM permeability increased with size possibly due to increased interaction between the positively charged surface groups with the anionic cell surface. G2 permeability increased with an increase in dendrimer concentration in the range of 50–300  $\mu\text{g/ml}$ . In this study, cytotoxicity assays were not performed to clarify whether the rank order of permeability was attributed to toxicity or not. Thus, the next logical step was to systematically evaluate the influence of size, charge, incubation time, and dendrimer concentration on their cytotoxicity and transepithelial transport across Caco-2 cell monolayers as a widely used in vitro model to assess the oral bioavailability of potential therapeutic agents (Artursson, 1990; Hilgers et al., 1990).

The influence of the physicochemical properties of PAMAM dendrimers (Table 14.2) on cytotoxicity and permeability across Caco-2 cells has been investigated (El-Sayed et al., 2002, 2003a; Kitchens et al., 2006; Kolhatkar et al., 2007). The permeability of the fluorescently labeled cationic PAMAM-NH<sub>2</sub> dendrimers changed as a function of incubation time, generation number, and concentration. Smaller dendrimers (G0–G2) had similar apical-to-basolateral (AB) permeability despite their different molecular weights. PAMAM permeability increased with time from 90

**Table 14.2** Structural features of selected PAMAM dendrimers studied for oral drug delivery.\*

Generation	Surface group	Molecular weight (Da)	Number of surface groups
G0	-NH <sub>2</sub>	517	4
G1	-NH <sub>2</sub>	1,430	8
G2	-NH <sub>2</sub>	3,256	16
G3	-NH <sub>2</sub>	6,909	32
G4	-NH <sub>2</sub>	14,215	64
G2	-OH	3,272	16
G3	-OH	6,909	32
G4	-OH	14,215	64
G-0.5	-COOH	436	4
G0.5	-COOH	1,269	8
G1.5	-COOH	2,935	16
G2.5	-COOH	6,267	32
G3.5	-COOH	12,931	64
G4.5	-COOH	26,258	128

\* Reported by the manufacturer, Dendritech, Inc., Midland, MI.



to 150 minutes (Figure 14.2A-B) and concentration from 1.0 to 10.0 mM (El-Sayed et al., 2002). Additionally, these smaller dendrimers exhibited higher permeability than G3 while exerting no toxicity at 1.0 mM toward Caco-2 cell monolayers. Lactate dehydrogenase (LDH) assay demonstrated that an increase in generation number, concentration, or incubation time

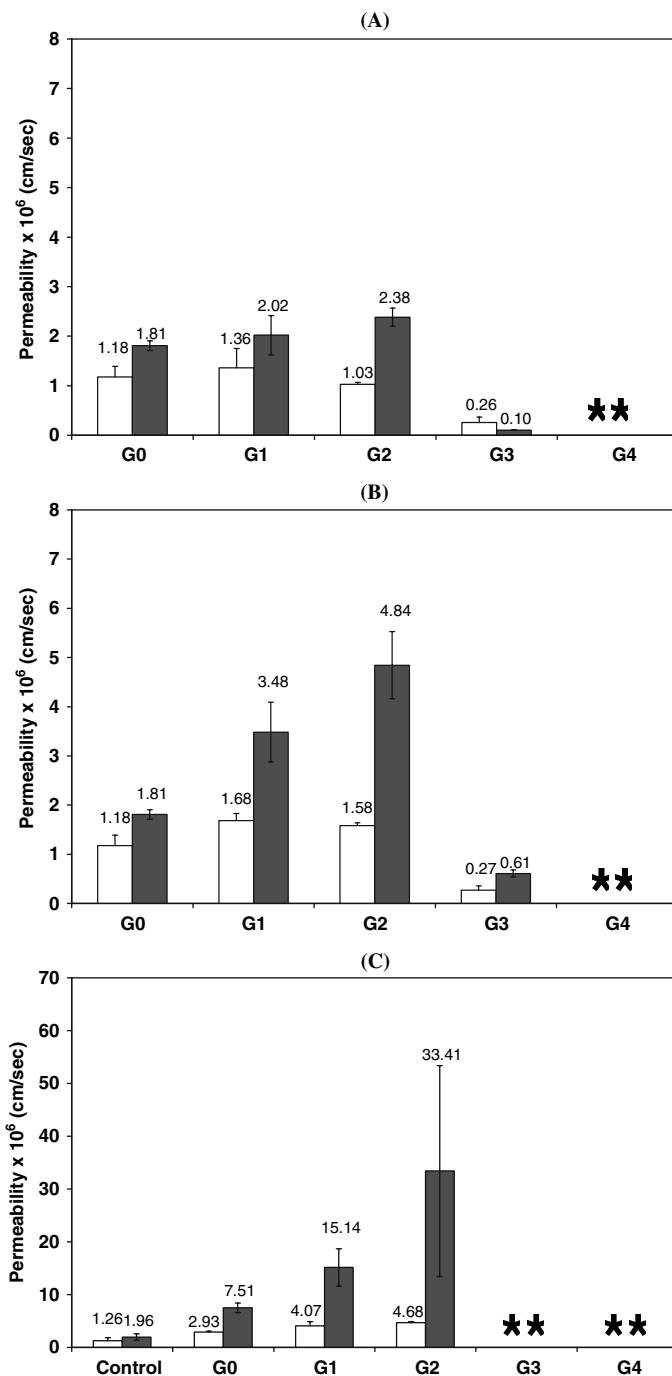


**Figure 14.2** AB (□) and BA (■) Caco-2 permeability of PAMAM dendrimers (G0–G4) at a donor concentration of 1.0 mM and incubation times of: (A) 90 minutes and (B) 150 minutes; and (C)  $^{14}\text{C}$ -mannitol at an incubation time of 210 minutes in the presence of 1.0 mM solution of PAMAM dendrimers (G0–G4). AB and BA permeability values are not reported (\*\*) at toxic incubation time points. Results are reported as mean  $\pm$  SEM ( $n = 9$ ). Adapted from El-Sayed et al. (2002) with permission from Elsevier.

resulted in an increase in cytotoxicity. The increase in cytotoxicity and permeability may be facilitated by the interaction between cationic amine groups of PAMAM dendrimers and negatively charged Caco-2 cell epithelia. This interaction is prolonged with an increase in time, and by increased surface charge density with an increase in concentration and generation number. This enhanced interaction may result in cell membrane perturbation by the cationic PAMAM dendrimers or tight junction modulation.

The influence of PAMAM dendrimers on the integrity and paracellular permeability of Caco-2 cell monolayers was investigated through transepithelial electrical resistance (TEER) measurements and the permeability of a known paracellular permeability marker,  $^{14}\text{C}$ -mannitol (El-Sayed et al., 2002, 2003a). TEER values decreased with an increase in cationic PAMAM-NH<sub>2</sub> generation number, donor concentration, and incubation time.  $^{14}\text{C}$ -mannitol permeability in the presence of dendrimers increased with PAMAM-NH<sub>2</sub> generation and concentration (Figure 14.2C) (El-Sayed et al., 2002). Neutral PAMAM-OH dendrimers did not significantly influence TEER compared to control conditions, nor significantly enhance  $^{14}\text{C}$ -mannitol permeability, whereas anionic PAMAM-COOH dendrimers had a generation-dependent effect on TEER and  $^{14}\text{C}$ -mannitol permeability (El-Sayed et al., 2003a). G-0.5, G0.5, G1.5, and G4.5 caused no significant decline in TEER values nor significantly enhanced  $^{14}\text{C}$ -mannitol permeability (at non-toxic conditions), whereas G2.5 and G3.5 caused a significant decline in TEER and significantly increased  $^{14}\text{C}$ -mannitol permeability compared to control values. The observed decrease in TEER values and increased mannitol permeability suggest PAMAM dendrimers enhance paracellular transport via tight junction modulation.

These initial studies demonstrated a size and charge window of PAMAM dendrimers that can traverse the epithelial barrier of the gut, as well as enhance drug transport. Recent studies focused on a systematic correlation between the effect of size and charge on PAMAM permeability across the intestinal barrier. It was demonstrated that PAMAM permeability is affected by dendrimer size among anionic dendrimers (G1.5–G3.5) and charge among dendrimers of similar size and different surface functionality (G2NH<sub>2</sub>, G2OH, G1.5COOH) (Kitchens et al., 2006). Permeability increased with an increase in generation among the PAMAM-COOH series without causing cytotoxicity (Figure 14.3). This data coupled with previous findings (Wiwattanapatapee et al., 2000) further confirm the potential of anionic PAMAM dendrimers as oral drug carriers. The influence of dendrimer surface charge on epithelial permeability was investigated while monitoring the  $^{14}\text{C}$ -mannitol flux. The rank order of dendrimer (Figure 14.3) and  $^{14}\text{C}$ -mannitol permeability (Figure 14.4), as well as their reduction in TEER (Figure 14.5), was G2NH<sub>2</sub> > G1.5COOH > G2OH. The effect of all tested PAMAM dendrimers on TEER, except G2NH<sub>2</sub>, was reversible after 24 hours. Other studies demonstrating the reversible effect of cationic and anionic dendrimers on Caco-2 cells (Jevprasesphant et al., 2003a) coupled with their non-toxic effects based on the WST-1 cytotoxicity assay (Kitchens et al., 2006) suggest the feasibility of the design and development of safe and effective oral drug carriers.

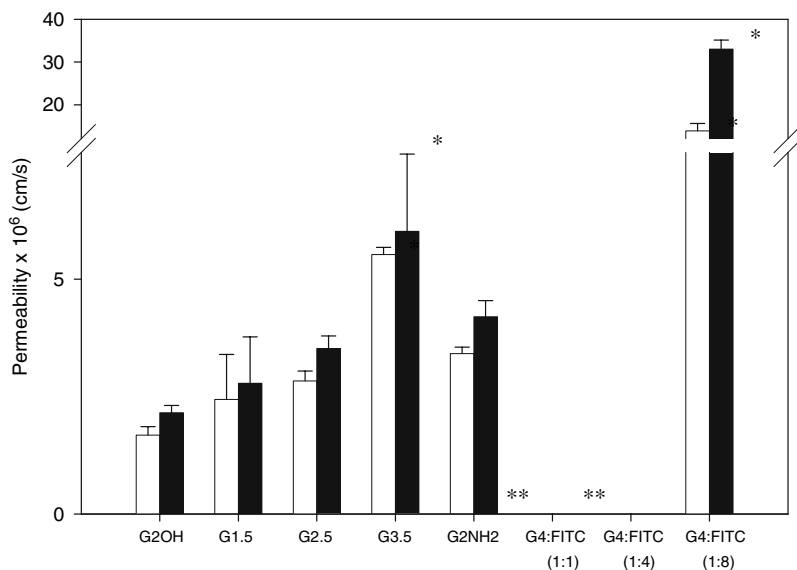


**Figure 14.3** The permeability of fluorescently labeled PAMAM dendrimers of donor concentration 1.0 mM across Caco-2 cell monolayers at incubation times of (□) 60 minutes and (■) 120 minutes. Permeability values are not reported (\*\*) for dendrimers that cause toxicity. Results are reported as mean  $\pm$  SEM ( $n = 9$ ). (\*) Denotes a significant difference in permeability compared to permeability of G2NH<sub>2</sub>, G2OH, G1.5COOH, and G2.5COOH dendrimers (G3.5COOH  $P < 0.05$ , G4NH<sub>2</sub>:FITC (1:8)  $P < 0.01$ ). Reprinted from Kitchens et al. (2006) (with permission from Springer).

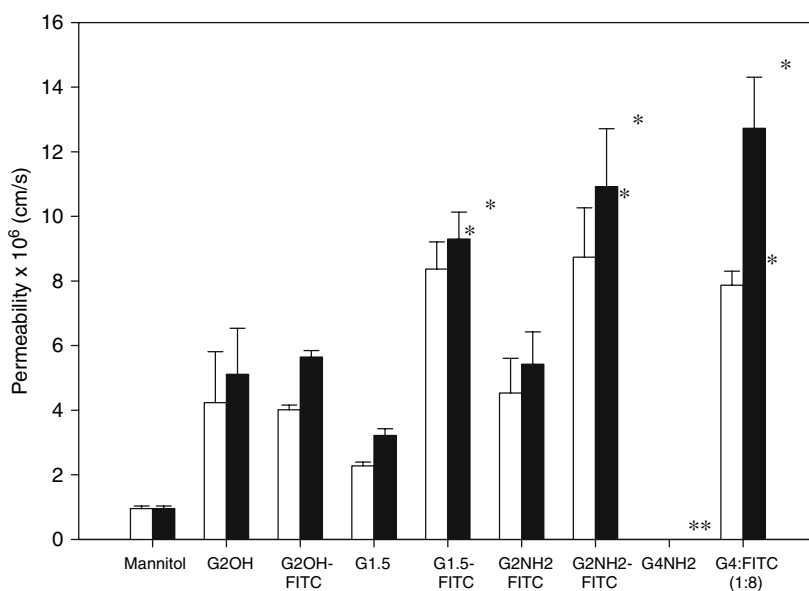


**Figure 14.4** The permeability of <sup>14</sup>C-mannitol (3.3  $\mu$ M) in the presence of fluorescently labeled and unlabeled PAMAM dendrimers of donor concentration 1.0 mM across Caco-2 cell monolayers at incubation times of (□) 60 minutes and (■) 120 minutes. Permeability values are not reported (\*\*) for dendrimers that cause toxicity. Results are reported as mean  $\pm$  SEM ( $n = 9$ ). (\*) Denotes a significant increase in permeability compared to control ( $P < 0.001$ ). Reprinted from Kitchens et al. (2006) (with permission from Springer).

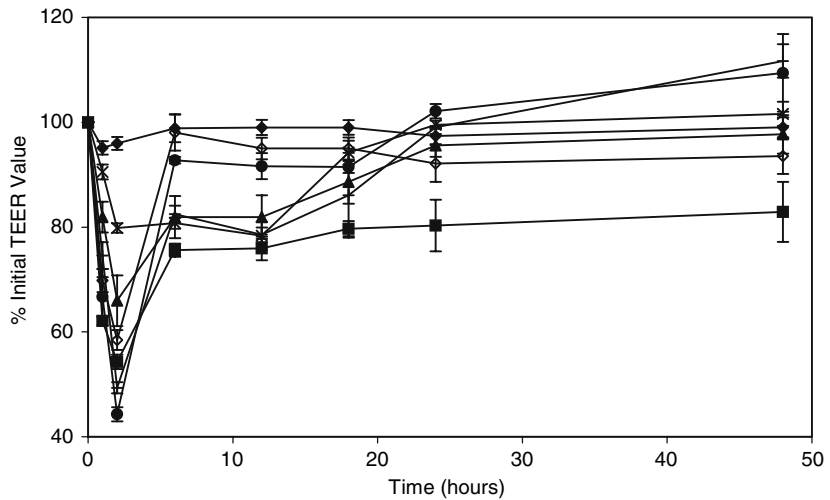


**Figure 14.5** Transepithelial electrical resistance of Caco-2 cells in the presence of fluorescently labeled PAMAM dendrimers as a function of time: (◆) HBSS transport medium, (■) G2NH<sub>2</sub>, (▲) G2OH, (×) G1.5COOH, (+) G2.5COOH, (●) G3.5COOH, (◇) G4NH<sub>2</sub>-FITC (1:8). Results are reported as mean ± SEM ( $n = 9$ ). Reprinted from Kitchens et al. (2006) (with permission from Springer).

#### **Influence of Surface Modification on Poly(amidoamine) Cytotoxicity and Permeability**

An interesting finding was <sup>14</sup>C-mannitol flux significantly increased in the presence of fluorescently labeled G2NH<sub>2</sub> and G1.5COOH dendrimers, where they caused a greater decline in TEER, relative to their unlabeled counterparts (Kitchens et al., 2006). G4NH<sub>2</sub> dendrimers were conjugated with FITC (as a model drug) at feed molar ratios of 1:1, 1:4, and 1:8 (G4NH<sub>2</sub>:FITC) to investigate how an incremental increase in conjugation would modify the toxicity and permeability of the dendrimers. The toxicity of G4NH<sub>2</sub> dendrimers reduced with an increase in FITC content (Table 14.3). G4NH<sub>2</sub>-FITC (1:8) displayed the highest relative permeability (Figure 14.3) with an increase in mannitol flux (Figure 14.4), most likely due to a higher degree of tight junctional modulation.

Other studies demonstrated surface modification of cationic PAMAM dendrimers with longer molecules such as lauroyl chains or PEG reduced their cytotoxicity in Caco-2 cells (Jevprasesphant et al., 2003b). Cell viability was based on the MTT assay, and the cytotoxicity of PAMAM dendrimers was a function of size, concentration, and surface charge (Jevprasesphant et al., 2003b). Anionic G2.5 and G3.5 dendrimers did not significantly reduce cell viability up to 1000 μM donor concentration and cationic G2 reduced cell viability at concentrations above 700 μM. G3 toxicity occurred when concentrations exceeded 10 μM, and G4 reduced cell viability at all donor concentrations tested. The cytotoxicity of PAMAM dendrimers decreased when they were modified with C<sub>12</sub> lauroyl chains or PEG molecules, which was indicated by increased IC<sub>50</sub> values when cationic dendrimers were modified with six lauroyl chains or four PEG molecules. The reduction in cytotoxicity can be explained by shielding of the positively

**Table 14.3.** Viability of Caco-2 cells measured with WST-1 assay reagent.\*

Concentration	0.01 mM	0.1 mM	1.0 mM
HBSS		100.0%	
G2NH <sub>2</sub>	80.3% ± 10.8%	78.0% ± 6.6%	77.3% ± 1.9%
G2NH <sub>2</sub> -FITC	88.5 ± 7.5%	92.5 ± 4.9%	86.8 ± 5.5%
G2OH	103.7 ± 10.1%	103.6 ± 7.9%	96.7 ± 3.3%
G2OH-FITC	104.1 ± 6.5%	97.8 ± 13.8%	98.8 ± 4.2%
G1.5COOH	100.5 ± 17.1%	110.3 ± 3.4%	105.4 ± 7.4%
G1.5COOH-FITC	107.2 ± 6.8%	99.5 ± 5.8%	111.8 ± 6.6%
G2.5COOH	109.1 ± 3.1%	91.6 ± 13.5%	108.3 ± 3.7%
G2.5COOH-FITC	104.3 ± 11.2%	99.7 ± 16.5%	106.7 ± 10.0%
G3.5COOH	90.7 ± 1.5%	88.6 ± 2.6%	86.8 ± 4.9%
G3.5COOH-FITC	108.1 ± 3.1%	107.0 ± 9.4%	101.7 ± 11.7%
G4NH <sub>2</sub>	66.7 ± 28.8%	60.2 ± 6.2%	38.1 ± 7.1%
G4NH <sub>2</sub> -FITC (1:1)	58.9 ± 4.3%	53.8 ± 9.8%	53.8 ± 10.4%
G4NH <sub>2</sub> -FITC (1:4)	85.1 ± 9.4%	76.8 ± 13.5%	56.3 ± 3.8%
G4NH <sub>2</sub> -FITC (1:8)	97.7 ± 4.8%	76.5 ± 3.6%	74.3 ± 4.3%
FITC	107.3 ± 35.7%	108.5 ± 40.0%	98.1 ± 38.5%
Triton X-100		30.4 ± 18.1%	

\*Results are reported as mean percentage ± standard deviation of the negative control, HBSS ( $n = 3$ ). Italicized cells indicate a significant reduction in cell viability compared to the negative control, HBSS, based upon a  $p$ -value < 0.05 using Student's  $t$ -test. Reprinted from Kitchens et al. (2006) (with permission from Springer).

charged amine groups to interact with negatively charged cell surface proteins (Jevprasesphant et al., 2003b). The permeabilities of surface-modified dendrimers with unmodified counterparts were compared (Jevprasesphant et al., 2003a). PAMAM permeability generally increased with an increase in the number of lipid chains and concentration. The only exception was observed for G2 dendrimers when the number of lauroyl chains increased from six to nine, where the permeability of G2L9 was lower than G2L6. This was explained by the self-association of this conjugate, since aggregation was facilitated by the small size of G2 and the increased number of hydrophobic chains. Furthermore, lauroyl-modified dendrimers did not reduce TEER values as much as unmodified dendrimers. These results correspond with the observations that PAMAM cytotoxicity reduced with the conjugation of lipid chains by reducing the interaction between the cationic surface groups and the cell membrane. It is well established that fatty acids enhance membrane permeability, possibly by opening tight junctions (Aungst, 2000), and increased hydrophobicity generally enhances uptake and transport through the gut (Florence, 1997). Together, the studies described above (Jevprasesphant et al., 2003a,b; Kitchens et al., 2006) clearly demonstrate that surface modification reduces the toxicity of cationic PAMAM dendrimers and enhances their permeability across Caco-2 cells (Jevprasesphant et al., 2003a,b; Kitchens et al., 2006).

Recently Kolhatkar et al. (2007) modified the surface of G2 and G4 dendrimers with acetic anhydride (Figure 14.6A) to determine if an optimal surface charge density can be achieved where PAMAM dendrimers possess minimal cytotoxicity without compromising their permeability. Cell

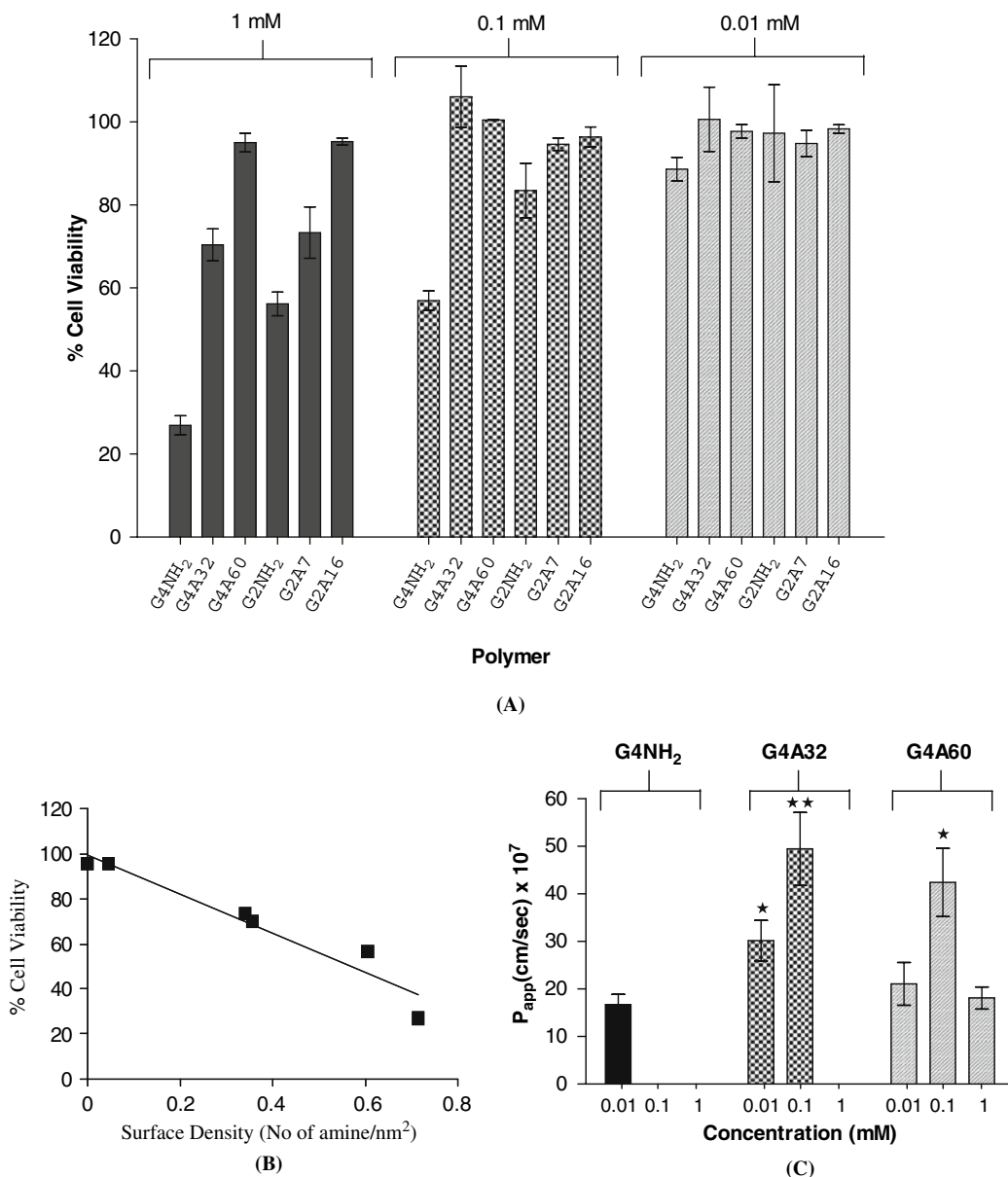


**Figure 14.6** (A) In vitro cell viability of Caco-2 cells after incubation with dendrimers for 3 hours. Results are reported as mean  $\pm$  SEM ( $n = 9$ ). (B) Relationship between cell viability and surface density. (C) Permeability of (■) G4NH<sub>2</sub>, (▨) G4A32, and (▩) G4A60 across Caco-2 cell monolayers after 120 min (G4Ax denotes generation 4 PAMAM-NH<sub>2</sub> dendrimers with  $x$  number of acetylated surface amine groups). Results are reported as mean  $\pm$  SEM ( $n = 6$ ). (\*) ( $p < 0.05$ ) and ( $p < 0.01$ ); (\*\*) denotes significant difference in permeability when compared to permeability of unmodified PAMAM dendrimer at 0.01 mM. (×) Permeability is not evaluated due to cytotoxicity. Adapted from Kolhatkar et al. (2007) (with permission from ACS Publications).

viability was at least 90% when cells were treated with partially and fully functionalized PAMAM dendrimers (0.1 mM) for 3 hours, suggesting partial modification is sufficient to reduce cytotoxicity (Figure 14.6A). At 1.0 mM, the toxic effects of PAMAM dendrimers decreased with an increase in surface acetylation, and a linear relationship was established between the surface density of amine groups and cytotoxicity (Figure 14.6B). A multi-regressional analysis (significant  $F < 0.001$ ;  $R^2 = 0.7$ ) was performed with the percentage cell viability as the dependant variable and surface density and concentration the independent variables, to give the following equation where  $C$  is concentration in mmol and  $SD_a$  is the surface density of amine groups (number of amine groups/nm<sup>2</sup>):

$$\% \text{ Cell Viability} = 15.5 \text{Log}(1/C) - 50.9SD_a + 87.6 \quad (1)$$

This equation describes cell viability as dependent on a combination of surface amine groups, dendrimer size, and concentration, and can be useful in predicting optimal surface modification to reduce PAMAM dendrimer toxicity (Kolhatkar et al., 2007). The AB permeability of non-toxic acetylated dendrimers was evaluated across Caco-2 cells. The permeability of both G4A32 and G4A60 at 0.01 mM was greater than that of unmodified G4, and a 1.5- and 2-fold enhancement of cellular permeability was achieved by increasing the G4A32 and G4A60 from 0.01 to 0.1 mM, respectively (Figure 14.6C).

Surface modification of PAMAM dendrimers also enhanced <sup>14</sup>C-mannitol permeability as a function of concentration and had a less drastic effect on TEER reduction compared to unmodified PAMAM dendrimers (Kolhatkar et al., 2007). TEER was reversible within 24 hours after dendrimer removal. The permeability enhancement of acetylated dendrimers could possibly be ascribed to a reduction of repulsive forces between surface amine groups, which would render the dendrimer structure more compact and result in increased permeability. Another possibility is that non-specific binding between dendrimers and the cell membrane may result in a relatively higher concentration of free dendrimer at the apical side of the membrane contributing to increased permeability (Kolhatkar et al., 2007). Further investigation revealed that surface modification of cationic PAMAM dendrimers leads to only modest decreases in cellular uptake compared to native dendrimer (Kolhatkar et al., 2007). Overall, these studies demonstrated acetylated PAMAM dendrimers had reduced cytotoxicity compared to unmodified dendrimers while maintaining appreciable permeability, therefore providing a window of opportunity for utilization of cationic PAMAM dendrimers in oral drug delivery.

### Transport Mechanisms and Intracellular Fate of PAMAM Dendrimers

Several studies have attempted to elucidate the transport mechanisms of PAMAM dendrimers (Duncan & Izzo, 2005; Kitchens et al., 2005). Temperature-dependent studies demonstrated the permeability of cationic, anionic (Figure 14.7), and lipid-modified dendrimers was lower at 4°C

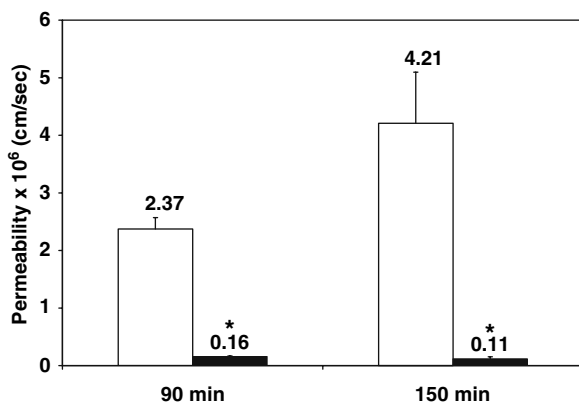


**Figure 14.7** AB permeability of G2 across Caco-2 cell monolayers at incubation times of 90 and 150 minutes at 37°C (□) and 4°C (■). Statistical difference at  $P < 0.05$  is denoted by (\*). Results are reported as mean  $\pm$  SEM. Reprinted from El-Sayed et al. (2003b) (with permission from Elsevier).

than observed at 37°C, suggesting the contribution of an energy-dependent process (El-Sayed et al., 2003b). Basolateral-to-apical (BA) permeability of PAMAM dendrimers was consistently greater than the corresponding AB permeability (El-Sayed et al., 2002, 2003a; Jevprasesphant et al., 2003a), thus the contribution of the P-gp efflux system to PAMAM transport was studied by measuring the permeability of  $^{14}\text{C}$ -paclitaxel, a known P-gp substrate, in the absence and presence of G2NH<sub>2</sub> (El-Sayed et al., 2003b). There were no significant differences in the permeability of  $^{14}\text{C}$ -paclitaxel in the presence of G2NH<sub>2</sub>, nor did the permeability of G2NH<sub>2</sub> change in the presence of  $^{14}\text{C}$ -paclitaxel, which suggested G2NH<sub>2</sub> is not a P-gp substrate (Figure 14.8). Additionally, the AB transport of propanolol, a poorly soluble P-gp substrate, increased while the BA transport decreased when propanolol was conjugated to G3NH<sub>2</sub> (D'Emanuele et al., 2004). This observation further demonstrates cationic dendrimers cannot be substrates for the P-gp efflux system since G3NH<sub>2</sub> enhanced the AB transport of propanolol. Finally, the application of palmitoyl carnitine, a typical absorption enhancer (Aungst, 2000), resulted in similar increases in the AB permeability of G2NH<sub>2</sub> and mannitol across Caco-2 cell monolayers (El-Sayed et al., 2003b). This observation, along with the observations that PAMAM dendrimers enhance mannitol permeability and decrease Caco-2 TEER through interaction with cellular tight junctions, suggest dendrimer transport is in part due to the paracellular route (El-Sayed et al., 2003b). Confocal laser scanning microscopy was used to visually confirm that PAMAM dendrimers open tight junctions (Kitchens et al., 2006). Caco-2 cells treated with PAMAM dendrimers for 2 hours displayed increased accumulation of the tight junctional protein occludin as evidenced by the disruptive staining pattern compared to control cells (Figure 14.9). Similar results were observed when cells were treated with rhodamine phalloidin to identify the actin protein. These data correspond to the observations that PAMAM dendrimers reduce TEER and increase  $^{14}\text{C}$ -mannitol permeability, and directly confirm that they contribute to the opening of tight junctions. Together these studies clearly suggested G2NH<sub>2</sub> is transported across Caco-2 cell monolayers by a combination of the paracellular pathway and an energy-dependent process, such as endocytosis, and that G2NH<sub>2</sub> is not a substrate for the P-gp efflux system.



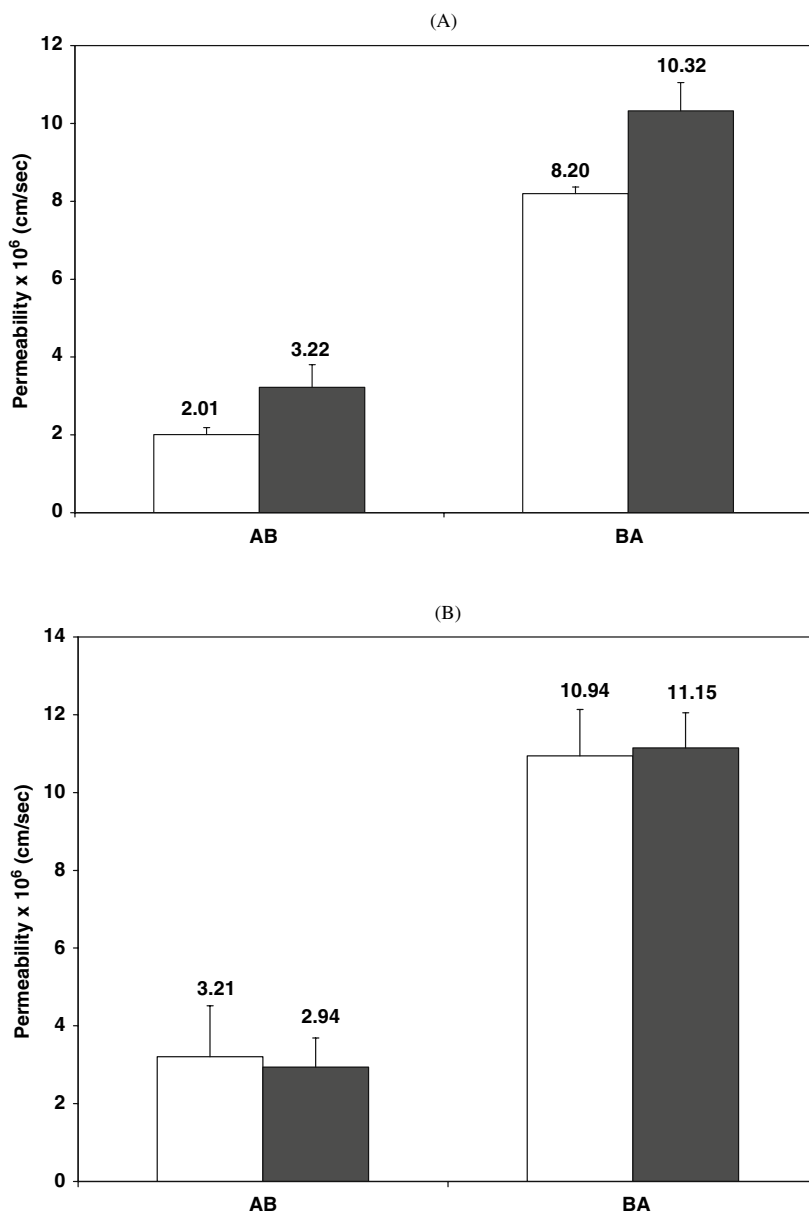


**Figure 14.8** (A) AB and BA permeability of <sup>14</sup>C-paclitaxel across Caco-2 cell monolayers in absence (□) and presence (■) of G2 (10.0 mM) at incubation time of 150 minutes. (B) AB and BA permeability of G2 (10.0 mM) across Caco-2 cell monolayers in absence (□) and presence (■) of paclitaxel (200 nM) at incubation time of 150 minutes. Results are reported as mean ± SEM. Reprinted from El-Sayed et al. (2003b) (with permission from Elsevier).

To further investigate the endocytosis of PAMAM dendrimers, their intracellular location was explored using various microscopy techniques. First, significant levels of FITC-labeled dendrimers were measured in Caco-2 cells after 3 hours treatment using flow cytometry and confocal

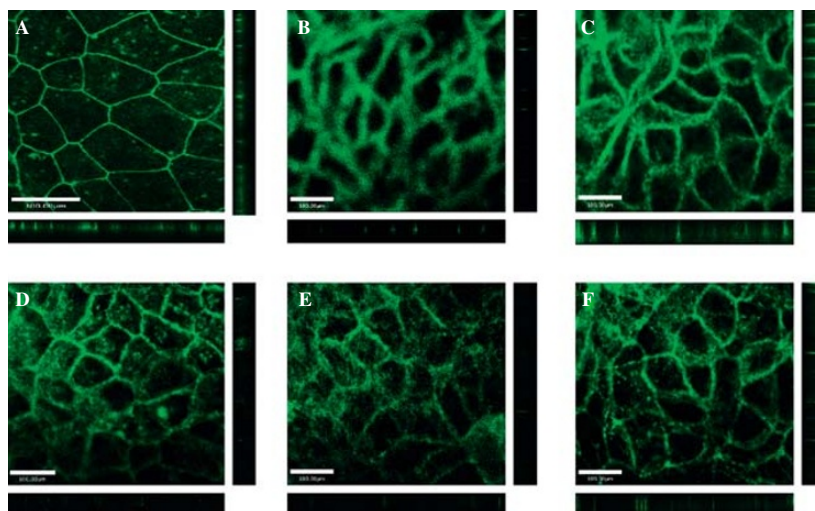


**Figure 14.9** Staining of the tight junction protein occludin. (A) Caco-2 cells with no polymer treatment. Caco-2 cells incubated for 120 minutes with 1.0 mM: (B) G2NH<sub>2</sub>; (C) G2OH, (D) G1.5COOH; (E) G2.5COOH; (F) G3.5COOH. Main panels illustrate the *xy* plane; horizontal bars illustrate the *xz* plane; vertical bars illustrate the *yz* plane. Scale bars equal 100.00  $\mu\text{m}$ . Reprinted from Kitchens et al. (2006) (with permission from Springer). (See Color Plate 19)

laser scanning microscopy indicating that the polymers were internalized within the cells and not adsorbed to the cell surface (Jevprasesphant et al., 2004). TEM was used to track the internalization process of dendrimer-gold nanocomplexes in Caco-2 cells. The nanocomposites were localized in vesicular compartments located below the apical membrane, presumably endosomes, and in multivesicular compartments throughout the cells. These observations suggested an endocytosis process contributes to dendrimer transport. To confirm these indirect observations, confocal laser scanning microscopy techniques were used to visualize the intracellular localization of dendrimers in Caco-2 cells, and quantify the extent of colocalization between PAMAM dendrimers and established endocytosis markers (Kitchens et al., 2007). Both cationic and anionic PAMAM dendrimers internalized within 20 minutes and colocalized with endocytosis markers clathrin, EEA-1, and LAMP-1 (Figure 14.10). Fluorescently labeled dendrimers colocalized with the early endosomal markers, anti-clathrin and anti-EEA1, greater than 70% after 20 and 60 minutes (Table 14.4), and colocalized to a lesser extent with the lysosomal marker, LAMP-1, which suggests PAMAM dendrimers are primarily localized in endosomal compartments. Interestingly, colocalization of G2NH<sub>2</sub> with LAMP-1 increased proportionally with time, suggesting lysosomal trafficking of cationic dendrimers is incubation time dependent. Similarly, colocalization of PAMAM dendrimers with EEA-1, specific to early endosomes, was high after 20 minutes, and reduced with time (Table 14.4). The confocal data confirmed that PAMAM dendrimers are localized in endosomal compartments, and dendrimer trafficking to secondary endosomes and lysosomes is time and surface charge dependent.

**Figure 14.10** Internalization of fluorescently labeled transferrin (250  $\mu\text{g}/\text{ml}$ ) and PAMAM dendrimers (100 nM) in Caco-2 cells after 20 minutes. The orange color in merged panels indicates colocalization with clathrin heavy chain, early endosomal antigen-1 (EEA-1), and lysosome-associated membrane protein-1 (LAMP-1). Main panels illustrate the  $xy$  plane; vertical panels illustrate the  $yz$  plane; horizontal panels illustrate the  $xz$  plane. Scale bars = 5  $\mu\text{m}$ . Adapted from Kitchens et al. (2007) (with permission from ACS Publications). (See Color Plate 20)

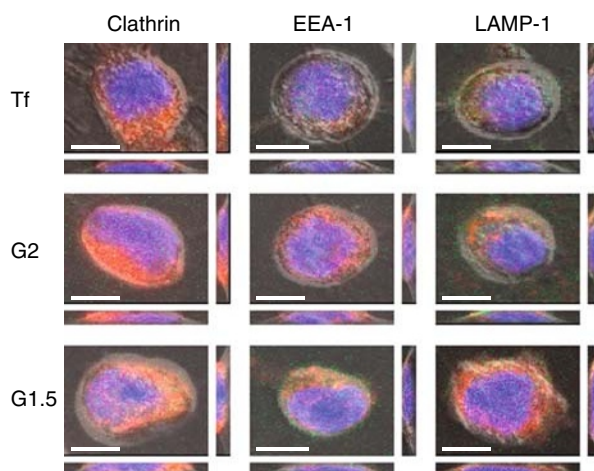


**Table 14.4** Extent of colocalization between transferrin and PAMAM dendrimers with endocytosis markers.\*

	Incubation time (min)	Clathrin	EEA-1	LAMP-1
Transferrin	20	80.3 $\pm$ 3.1%	70.4 $\pm$ 7.0%	63.9 $\pm$ 7.3%
	60	83.4 $\pm$ 0.2%	79.6 $\pm$ 0.4%	57.0 $\pm$ 8.6%
G2NH <sub>2</sub>	20	74.3 $\pm$ 5.2%	76.7 $\pm$ 3.4%	37.4 $\pm$ 5.9%
	60	73.7 $\pm$ 3.8%	72.1 $\pm$ 0.4%	59.0 $\pm$ 5.2%
G1.5COOH	20	70.8 $\pm$ 3.9%	60.1 $\pm$ 6.8%	58.7 $\pm$ 2.0%
	60	75.3 $\pm$ 1.2%	53.8 $\pm$ 9.7%	48.9 $\pm$ 1.3%

\*Colocalization coefficients ( $M_x$ ) were calculated using the following equation:

$$M_x = \frac{\sum_i x_i \text{coloc}}{\sum_i x_i}$$

where  $x_i \text{coloc}$  is the value of voxel  $i$  of the overlapped FITC and Alexa Fluor 568<sup>®</sup> components, and  $x_i$  is the value of voxel  $i$  of the FITC component.  $M_x$  values are reported as mean  $\pm$  standard error of the mean ( $n = 6$ ). Reprinted from Kitchens et al. (2007) (with permission from ACS Publications).

### Microvascular Extravasation of Poly(amidoamine) Dendrimers

Once drugs and macromolecules are absorbed orally, they are distributed throughout the circulatory system and must extravasate across the microvascular endothelium of capillary walls to reach the site of therapeutic action in neighboring interstitial tissues (El-Sayed et al., 2001; Takakura et al., 1998). Previous studies investigated the influence of dendrimer size and molecular weight on their microvascular extravasation (El-Sayed et al., 2001). The extravasation time of a series of fluorescently labeled PAMAM-NH<sub>2</sub> dendrimers and PEG (MW = 6000 Da) was investigated across the microvascular endothelium in the cremaster muscle of male Syrian hamsters using intravital microscopy techniques. The extravasation time was measured as the time required for fluorescence intensity in interstitial tissue to reach 90% the fluorescence intensity in the neighboring

microvasculature. Extravasation time increased exponentially with the increase in PAMAM dendrimer molecular weight and size, and the rank order of extravasation time was  $G0 < G1 < G2 < G3 < G4 < \text{PEG}$ , ranging from 143.9 to 453.9 seconds. This size-dependent selectivity is in part due to the increased exclusion of PAMAM-NH<sub>2</sub> dendrimers from the endothelial pores, 4-5 nm in radius, as dendrimer size (1.5–4.5 nm) and hydrodynamic volume increased (El-Sayed et al., 2001).

PEG had the earliest size-exclusion elution volume compared to the dendrimers, which indicates PEG had a greater hydrodynamic volume and consequently longer extravasation time than PAMAM dendrimers. The microvascular endothelium is lined with the glycocalyx layer, which is composed of negatively charged sulfated glycosaminoglycan (Adamson & Clough, 1992). The observed extravasation of PAMAM-NH<sub>2</sub> dendrimers and PEG molecules may also be a function of the electrostatic interactions between the polymers and the negatively charged endothelium. PAMAM-NH<sub>2</sub> dendrimers are positively charged at physiological pH, whereas PEG molecules are neutral. As a result, the electrostatic interaction between PAMAM-NH<sub>2</sub> dendrimers and the negatively charged glycocalyx lining was more favorable compared to the neutral PEG molecules, which led to the faster extravasation time observed for PAMAM-NH<sub>2</sub> dendrimers compared to PEG. Overall, this study demonstrated that an increase in molecular weight and size of polymers results in increased extravasation time across the microvascular endothelium. Molecular geometry and surface charge also influence the microvascular extravasation of water-soluble polymers across the endothelial barrier, in which compact, spherical, positively charged PAMAM dendrimers have shorter extravasation times than random-coiled, neutral PEG chains. It must be noted that in this study the uptake of polymers by tissues is a function of size and charge and its influence over extravasation time indeed warrants further consideration.

## Conclusions and Future Directions

The potential of PAMAM dendrimers as oral drug delivery carriers has been demonstrated by their appreciable permeability and uptake across the intestinal epithelial barrier, given their macromolecular nature. Earlier studies demonstrated that dendrimers could be administered as oral formulations since they are rapidly absorbed in the GI tract and perfuse to the circulatory system. Further studies demonstrated cationic PAMAM dendrimers extravasate across the microvascular endothelium. The biocompatibility and transport of PAMAM dendrimers across the epithelial barrier demonstrate a size and charge window where PAMAM dendrimers can have utility in drug delivery applications. To lessen the toxic effects of cationic PAMAM dendrimers, it is possible to modify the surface amine groups with inert, hydrophobic moieties that do not compromise, and in some cases enhance, dendrimer permeability. Mechanistic studies suggested PAMAM dendrimers open the tight junctions and are endocytosed leading to their own enhanced permeability. Together these studies demonstrate the potential of PAMAM dendrimers in the oral delivery of bioactive agents for systemic absorption. The next logical step in these

studies is to conjugate specific potent drugs for translocation across the GI tract and absorption to the blood circulation for targeted delivery to distant sites. The challenges remaining are appropriate conjugation (or complexation) strategies to facilitate delivery to the target sites. Further mechanistic studies can delineate the kinetics of subcellular localization and transcytosis. Such delineation can open new avenues for sub- or transcellular delivery of bioactive agents. The mechanisms by which PAMAM dendrimers open the tight junctions are not well understood. Finally, pre-clinical and clinical development of orally bioavailable dendrimers require a battery of biocompatibility, stability, transport, biodistribution, and efficacy studies depending on the type of carrier, cargo, and targeting strategies.

*Acknowledgments.* Financial support was in part provided by the National Institute of General Medical Sciences National Research Service Award predoctoral fellowship to Kelly Kitchens (F31-GM67278) and a grant from the National Institutes of Health (RO1EB007470).

## Abbreviations

Abbreviations: Full name:

1B4M	<i>p</i> -Isothiocyanatobenzyl)-6-methyl-diethylenetriamine pentaacetic acid
AB	Apical-to-basolateral
BA	Basolateral-to-apical
BRI	Biomolecular Research Institute
CAT	Chloramphenicol acetyl-transferase
CT	Computed topography
Da	Daltons
DAB	Diaminobutane
DMPC	1,2-Dimyristoyl- <i>sn</i> -glycero-3-phosphocholine
DNA	Deoxyribonucleic acid
DTPA	Diethylenetriaminepentaacetic acid
EEA-1	Early endosomal antigen 1
FITC	Fluorescein isothiocyanate
G	Generation
Gd	Gadolinium
GI	Gastrointestinal
HSV-2	Herpes simplex virus type 2
ID/g	Injected dose per gram
IR	Infra-red
LAMP-1	Lysosome-associated membrane protein 1
LDH	Lactate dehydrogenase
MALDI-TOF	Matrix-assisted laser desorption ionization time of flight
MDCK	Madin–Darby canine kidney
MRI	Magnetic resonance imaging
MTT	3-(4,5-Dimethylthiazole-2-yl)-2,5-diphenyltetrazolium bromide
NMR	Nuclear magnetic resonance

$P_{app}$	Apparent permeability
PAGE	Polyacrylamide gel electrophoresis
PAMAM	Poly(amidoamine)
PEG	Poly(ethylene glycol)
PEI	Poly(ethyleneimine)
PEO	Poly(ethylene oxide)
P-gp	P-glycoprotein
PPI	Poly(propyleneimine)
PVA	Poly(vinyl alcohol)
SANS	Small-angle neutron scattering
SAXS	Small-angle X-ray scattering
SDS	Sodium dodecyl sulfate
TEER	Transepithelial electrical resistance
TEM	Transmission electron microscopy
TNF- $\alpha$	Tumor necrosis factor

## References

- Adamson, R. H., & Clough, G. (1992). Plasma proteins modify the endothelial cell glycocalyx of frog mesenteric microvessels. *J Physiol*, *445*, 473–486.
- Artursson, P. (1990). Epithelial transport of drugs in cell culture. I: A model for studying the passive diffusion of drugs over intestinal absorptive (Caco-2) cells. *J Pharm Sci*, *79*(6), 476–482.
- Aulenta, F., Drew, M. G., Foster, A., Hayes, W., Rannard, S., Thornthwaite, D. W., Worrall, D. R., Youngs, T. G. (2005). Synthesis and characterization of fluorescent poly (aromatic amide) dendrimers. *J Org Chem*, *70*(1), 63–78.
- Aungst, B. J. (2000). Intestinal permeation enhancers. *J Pharm Sci*, *89*(4), 429–442.
- Bayele, H. K., Ramaswamy, C., Wilderspin, A. F., Srai, K. S., Toth, I., & Florence, A. T. (2006). Protein transduction by lipidic peptide dendrimers. *J Pharm Sci*, *95*(6), 1227–1237.
- Behr, J. P. (1994). Gene transfer with synthetic cationic amphiphiles: Prospects for gene therapy. *Bionconjug Chem*, *5*(5), 382–389.
- Bielinska, A., Kukowska-Latallo, J. F., Johnson, J., Tomalia, D. A., & Baker, J. R., Jr. (1996). Regulation of in vitro gene expression using antisense oligonucleotides or antisense expression plasmids transfected using starburst PAMAM dendrimers. *Nucleic Acids Res*, *24*(11), 2176–2182.
- Boas, U., Karlsson, A. J., de Waal, B. F., Meijer, E. W. (2001). Synthesis and properties of new thiourea-functionalized poly (propylene imine) dendrimers and their role as hosts for urea functionalized guests. *J Org Chem*, *66*(6), 2136–2145.
- Bourne, N. (2000). Dendrimers, a new class of candidate topical microbicides with activity against herpes simplex virus infection. *Antimicrob Agents Chemother*, *44*(9), 2471–2474.
- Brauge, L., Magro, G., Caminade, A. M., & Majoral, J. P. (2001). First divergent strategy using two AB(2) unprotected monomers for the rapid synthesis of dendrimers. *J Am Chem Soc*, *123*(27), 6698–6699.
- Brothers II, H. M., Piehler, I. T., & Tomalia, D. A. (1998). Slab-gel and capillary electrophoretic characterization of polyamidoamine dendrimers. *J Chromatogr A*, *814*(1–2), 233–246.
- Caminade, A. M., Laurent, R., & Majoral, J. P. (2005). Characterization of dendrimers. *Adv Drug Del Rev*, *57*(15), 2130–2146.

- Chai, M., Niu, Y., Youngs, W. J., Rinaldi, P.L. (2001). Structure and conformation of DAB dendrimers in solution via multidimensional NMR techniques. *J Am Chem Soc*, 123(20), 4670–4678.
- Chai, M., Pi, Z., Tessier, C., & Rinaldi, P. L. (1999). Preparation of carbosilane dendrimers and their characterization using  $^1\text{H}/^{13}\text{C}/^{29}\text{Si}$  triple resonance 3D NMR methods. *J Am Chem Soc*, 121(2), 273–279.
- Chauhan, A. S., Sridevi, S., Chalasani, K. B., Jain, A. K., Jain, S. K., & Jain, N. K. (2003). Dendrimer-mediated transdermal delivery: Enhanced bioavailability of indomethacin. *J Control Release*, 90(3), 335–343.
- Chen, H. T., Neerman, M. F., Parrish, A. R., & Simanek, E. E. (2004). Cytotoxicity, hemolysis, and acute in vivo toxicity of dendrimers based on melamine, candidate vehicles for drug delivery. *J Am Chem Soc*, 126, 10044–10048.
- Choe, Y. H., Conover, C. D., Wu, D., Royzen, M., Gervacio, Y., & Borowski, V. (2002). Anticancer drug delivery systems: Multi-loaded N4-acyl poly(ethylene glycol) prodrugs of ara-C. II. Efficacy in ascites and solid tumors. *J Control Release*, 79(1–3), 55–70.
- Choi, Y. S., Thomas, T., Kotlary, A., Islam, M. T., & Baker, J. R. (2005). Synthesis and functional evaluation of DNA-assembled polyamidoamine dendrimer clusters for cancer cell-specific targeting. *Chem Biol*, 12(1), 35–43.
- Cloninger, M. J. (2002). Biological applications of dendrimers. *Curr Opin Chem Biol*, 6(6), 742–748.
- D'Emanuele, A., & Attwood, D. (2005). Dendrimer-drug interactions. *Adv Drug Deliv Rev*, 57(15), 2147–2162.
- D'Emanuele, A., Jevprasesphant, R., Penny, J., & Attwood, D. (2004). The use of a dendrimer-propranolol prodrug to bypass efflux transporters and enhance oral bioavailability. *J Control Release*, 95(3), 447–453.
- DeLong, R., Stephenson, K., Loftus, T., Fisher, M., Alahari, S., Nolting, A., & Juliano, R. L. (1997). Characterization of complexes of oligonucleotides with polyamidoamine starburst dendrimers and effects on intracellular delivery. *J Pharm Sci*, 86(6), 762–764.
- Dufes, C., Keith, W. N., Bilsland, A., Proutski, I., Uchegbu, I. F., & Schatzlein, A. G. (2005a). Synthetic anticancer gene medicine exploits intrinsic antitumor activity of cationic vector to cure established tumors. *Cancer Res*, 65(18), 8079–8084.
- Dufes, C., Uchegbu, I. F., & Schatzlein, A. G. (2005b). Dendrimers in gene delivery. *Adv Drug Deliv Rev*, 57(15), 2177–2202.
- Duncan, R., & Izzo, L. (2005). Dendrimer biocompatibility and toxicity. *Adv Drug Deliv Rev*, 57(15), 2215–2237.
- Duncan, R., & Spreafico, F. (1994). Polymer conjugates. Pharmacokinetic considerations for design and development. *Clin Pharmacokinet*, 27(4), 290–306.
- Dunphy, I., Vinogradov, S. A., & Wilson, D. F. (2002). Oxyphor R2 and G2: Phosphors for measuring oxygen by oxygen-dependent quenching of phosphorescence. *Anal Biochem*, 310(2), 191–198.
- El-Sayed, M., Ginski, M., Rhodes, C., & Ghandehari, H. (2002). Transepithelial transport of poly(amidoamine) dendrimers across Caco-2 cell monolayers. *J Control Release*, 81(3), 355–365.
- El-Sayed, M., Ginski, M., Rhodes, C., & Ghandehari, H. (2003a). Influence of surface chemistry of poly(amidoamine) dendrimers on Caco-2 cell monolayers. *J Bioactive Compat Poly*, 18, 7–22.
- El-Sayed, M., Rhodes, C. A., Ginski, M., & Ghandehari, H. (2003b). Transport mechanism(s) of poly(amidoamine) dendrimers across Caco-2 cell monolayers. *Int J Pharm*, 265(1–2), 151–157.
- El-Sayed, M., Kiani, M. F., Naimark, M. D., Hikal, A. H., & Ghandehari, H. (2001). Extravasation of poly(amidoamine) (PAMAM) dendrimers across microvascular network endothelium. *Pharm Res*, 18(1), 23–28.

- Esfand, R., & Tomalia, D. A. (2001). Poly (amidoamine) (PAMAM) dendrimers: From biomimicry to drug delivery and biomedical applications. *Drug Discov Today*, 6(8), 427–436.
- Felder, T., Schalley, C. A., Fakhnabavi, H., & Lukin, O. (2005). A combined ESI- and MALDI-MS(/MS) study of peripherally persulfonated dendrimers: False negative results by MALDI-MS and analysis of defects. *Chemistry*, 11(19), 5625–5636.
- Fischer, D., Li, Y., Ahlemeyer, B., Krieglstein, J., & Kissel, T. (2003). In vitro cytotoxicity testing of polycations: Influence of polymer structure on cell viability and hemolysis. *Biomaterials*, 24(7), 1121–1131.
- Florence, A. T. (1997). The oral absorption of micro- and nanoparticles: Neither exceptional nor unusual. *Pharm Res*, 14, 259–266.
- Florence, A. T., Sakthivel, T., & Toth, I. (2000). Oral uptake and translocation of a polylysine dendrimer with a lipid surface. *J Control Release*, 65(1–2), 253–259.
- Fu, Y., Nitecki, D. E., Maltby, D., Simon, G. H., Berejnoi, K., Raatschen, H. J., Yeh, B. M., Shames, D. M., & Brasch, R. C. (2006). Dendritic iodinated contrast agents with PEG-cores for CT imaging: Synthesis and preliminary characterization. *Bioconjug Chem*, 17(4), 1043–1056.
- Grinstaff, M. W. (2002). Biodendrimers: New polymeric biomaterials for tissue engineering. *Chemistry*, 8(13), 2838–2846.
- Haensler, J., & Szoka, F. C., Jr. (1993). Polyamidoamine cascade polymers mediate efficient transfection of cells in culture. *Bioconjug Chem*, 4(5), 372–379.
- Halford, B. (2005). Dendrimers branch out. *Chem Eng News*, 83, 30–36.
- Hawker, C. J., & Frechet, J. M. J. (1990). Preparation of polymers with controlled molecular architecture. A new convergent approach to dendritic macromolecules. *J Am Chem Soc*, 112(21), 7638–7647.
- Hilgers, A. R., Conradi, R. A., & Burton, P. S. (1990). Caco-2 cell monolayers as a model for drug transport across the intestinal mucosa. *Pharm Res*, 7(9), 902–910.
- Hobbs, S. K., Monsky, W. L., Yuan, F., Roberts, W. G., Griffith, L., Torchilin, V. P., Jain, & R. K. (1998). Regulation of transport pathways in tumor vessels: Role of tumor type and microenvironment. *Proc Natl Acad Sci USA*, 95(8), 4607–4612.
- Hong, M. Y., Kim, Y. J., Lee, J. W., Kim, K., Lee, J. H., Yoo, J. S., Bae, S. H., Choi, B. S., & Kim, H. S. (2004a). Synthesis and characterization of tri(ethylene oxide)-attached poly(amidoamine) dendrimer layers on gold. *J Colloid Interface Sci*, 274(1), 41–48.
- Hong, S., Leroueil, P. R., Janus, E. K., Peters, J. L., Kober, M. M., Islam, M. T., Orr, B. G. Baker, J. R., Jr., & Banaszak Holl, M. M. (2006). Interaction of polycationic polymers with supported lipid bilayers and cells: Nanoscale hole formation and enhanced membrane permeability. *Bioconjug Chem*, 17(3), 728–734.
- Hong, S., Bielinska, A. U., Mecke, A., Keszler, B., Beals, J. L., Shi, X., Balogh, L., Orr, B. G., Baker, J. R., Jr., & Banaszak Holl, M. M. (2004b). Interaction of poly(amidoamine) dendrimers with supported lipid bilayers and cells: Hole formation and the relation to transport. *Bioconjug Chem*, 15(4), 774–782.
- Huang, Q. R., Dubin, P. L., Lal, J., Moorefield, C. N., & Newkome, G. R. (2005). Small-angle neutron scattering studies of charged carboxyl-terminated dendrimers in solutions. *Langmuir*, 21(7), 2737–2742.
- Hughes, J. A., Aronsohn, A. I., Avrutskaya, A. V., & Juliano, R. L. (1996). Evaluation of adjuvants that enhance the effectiveness of antisense oligodeoxynucleotides. *Pharm Res*, 13(3), 404–410.
- Hummelen, J. C., Van Dongen, J. L. J., & Meijer, E. W. (1997). Electrospray mass spectrometry of poly(propylene imine) dendrimers – the issue of dendritic purity or polydispersity. *Chem Eur J*, 3(9), 1489–1493.



- Ihre, H. R., Padilla De Jesus, O. L., Szoka, F. C., Jr., & Frechet, J. M. (2002). Polyester dendritic systems for drug delivery applications: Design, synthesis, and characterization. *Bioconjug Chem*, 13(3), 443–452.
- Irvine, J. D., Takahashi, L., Lockhart, K., Cheong, J., Tolan, J. W., Selick, H. E., & Grove, J. R. (1999). MDCK (Madin-Darby Canine Kidney) cells: A tool for membrane permeability screening. *J Pharm Sci*, 88(1), 28–33.
- Jackson, C. L., Chanzy, H. D., Booy, F. P., Drake, B. J., Tomalia, D. A., Bauer, B. J., & Amis, E. J. (1998). Visualization of dendrimer molecules by transmission electron microscopy (TEM): Staining methods and cryo-TEM of vitrified solutions. *Macromolecules*, 31(18), 6259–6265.
- Jevprasesphant, R., Penny, J., Attwood, D., & D'Emanuele, A. (2004). Transport of dendrimer nanocarriers through epithelial cells via the transcellular route. *J Control Release*, 97(2), 259–267.
- Jevprasesphant, R., Penny, J., Attwood, D., McKeown, N. B., & D'Emanuele, A. (2003a). Engineering of dendrimer surfaces to enhance transepithelial transport and reduce cytotoxicity. *Pharm Res*, 20(10), 1543–1550.
- Jevprasesphant, R., Penny, J., Jalal, R., Attwood, D., McKeown, N. B., & D'Emanuele, A. (2003b). The influence of surface modification on the cytotoxicity of PAMAM dendrimers. *Int J Pharm*, 252(1–2), 263–266.
- Jiang, Y. H., Emau, P., Cairns, J. S., Flanary, L., Morton, W. R., McCarthy, T. D., & Tsai, C.C. (2005). SPL7013 gel as a topical microbicide for prevention of vaginal transmission of SHIV89.6p in macaques. *AIDS Res Hum Retroviruses*, 21(3), 207–213.
- Juliano, R. L. (2006). Intracellular delivery of oligonucleotide conjugates and dendrimer complexes. *Ann NY Acad Sci*, 1082, 18–26.
- Kang, H., DeLong, R., Fisher, M. H., & Juliano, R. L. (2005). Tat-conjugated PAMAM dendrimers as delivery agents for antisense and siRNA oligonucleotides. *Pharm Res*(12), 22, 2099–2106.
- Kannan, S., Kolhe, P., Raykova, V., Glibatec, M., Kannan, R. M., Lieh-Lai, M., & Bassett, D. (2004). Dynamics of cellular entry and drug delivery by dendritic polymers into human lung epithelial carcinoma cells. *J Biomater Sci Polym Ed*, 15(3), 311–330.
- Karoonuthaisiri, N., Titiyevskiy, K., & Thomas, J. L. (2003). Destabilization of fatty acid-containing liposomes by polyamidoamine dendrimers. *Colloids Surf B Biointerfaces*, 27(24), 365–375.
- Khandare, J., Kolhe, P., Pillai, O., Kannan, S., Lieh-Lai, M., & Kannan, R. M. (2005). Synthesis, cellular transport, and activity of polyamidoamine dendrimer-methylprednisolone conjugates. *Bioconjug Chem*, 16(2), 330–337.
- Kim, T. I., Seo, H. J., Choi, J. S., Jang, H. S., Baek, J. U., Kim, K., & Park, J. S. (2004). PAMAM-PEG-PAMAM: Novel triblock copolymer as a biocompatible and efficient gene delivery carrier. *Biomacromolecules*, 5(6), 2487–2492.
- Kitchens, K. M., El-Sayed, M. E., & Ghandehari, H. (2005). Transepithelial and endothelial transport of poly (amidoamine) dendrimers. *Adv Drug Deliv Rev*, 57(15), 2163–2176.
- Kitchens, K. M., Foraker, A. B., Kolhatkar, R. B., Swaan, P. W., & Ghandehari, H. (2007). Endocytosis and interaction of poly (amidoamine) dendrimers with Caco-2 cells. *Pharmaceutical Research*, 24:2138–2145.
- Kitchens, K. M., Kolhatkar, R. B., Swaan, P. W., Eddington, N. D., & Ghandehari, H. (2006). Transport of poly(amidoamine) dendrimers across Caco-2 cell monolayers: Influence of size, charge and fluorescent labeling. *Pharm Res*, 23(12), 2818–2826.
- Kobayashi, H., & Brechbiel, M. W. (2005). Nano-sized MRI contrast agents with dendrimer cores. *Adv Drug Deliv Rev*, 57(15), 2271–2286.

- Kobayashi, H., Kawamoto, S., Saga, T., Sato, N., Hiraga, A., Ishimori, T., Konishi, J., Togashi, K., & Brechbiel, M. W. (2001a). Positive effects of polyethylene glycol conjugation to generation-4 polyamidoamine dendrimers as macromolecular MR contrast agents. *Magn Reson Med*, 46(4), 781–788.
- Kobayashi, H., Sato, N., Kawamoto, S., Saga, T., Hiraga, A., Haque, T. L., Ishimori, T., Konishi, J., Togashi, K., & Brechbiel, M. W. (2001b). Comparison of the macromolecular MR contrast agents with ethylenediamine-core versus ammonia-core generation-6 polyamidoamine dendrimer. *Bioconjug Chem*, 12(1), 100–107.
- Kolhatkar, K., Kitchens, K. M., Swaan, P. & Ghandehari, H. (2007), Surface acetylation of poly(amidoamine) (PAMAM) dendrimers decreases cytotoxicity while maintaining membrane permeability, *Bioconjugate Chemistry*, 18, 2054–2060.
- Kolhe, P., Khandare, J., Pillai, O., Kannan, S., Lieh-Lai, M., & Kannan, R. M. (2006). Preparation, cellular transport, and activity of polyamidoamine-based dendritic nanodevices with a high drug payload. *Biomaterials*, 27(4), 660–669.
- Kolhe, P., Khandare, J., Pillai, O., Kannan, S., Lieh-Lai, M., & Kannan, R. (2004). Hyperbranched polymer-drug conjugates with high drug payload for enhanced cellular delivery. *Pharm Res*, 21(12), 2185–2195.
- Kolhe, P., Misra, E., Kannan, R. M., Kannan, S., & Lieh-Lai, M. (2003). Drug complexation, in vitro release and cellular entry of dendrimers and hyperbranched polymers. *Int J Pharm*, 259(1–2), 143–160.
- Konda, S. D., Aref, M., Brechbiel, M., & Wiener, E. C. (2000). Development of a tumor-targeting MR contrast agent using the high-affinity folate receptor: Work in progress. *Invest Radiol*, 35(1), 50–57.
- Langereis, S., de Lussanet, Q. G., van Genderen, M. H., Meijer, E. W., Beets-Tan, R. G., Griffioen, A. W., van Engelshoven, J. M., & Backes, W. H. (2006). Evaluation of Gd(III)DTPA-terminated poly(propylene imine) dendrimers as contrast agents for MR imaging. *NMR Biomed*, 19(1), 133–141.
- Launay, N., Caminade, A. M., & Majoral, J. P. (1995). Synthesis and reactivity of unusual phosphorus dendrimers. A useful divergent growth approach up to the seventh generation. *J Am Chem Soc*, 117(11), 3282–3283.
- Lee, C. C., MacKay, J. A., Frechet, J. M., & Szoka, F. C. (2005). Designing dendrimers for biological applications. *Nat Biotechnol*, 23(12), 1517–1526.
- Liu, M., & Frechet, J. M. (1999). Designing dendrimers for drug delivery. *Pharm Sci Technol Today*, 2(10), 393–401.
- Liu, M., Kono, K., & Frechet, J. M. (2000). Water-soluble dendritic unimolecular micelles: Their potential as drug delivery agents. *J Control Release*, 65(1–2), 121–131.
- Loup, C., Zanta, M. A., Caminade, A. M., Majoral, J. P., & Meunier, B. (1999). Preparation of water soluble cationic phosphorous containing dendrimers as DNA transfecting agents. *Chem Eur J*, 5(12), 3644–3650.
- Luo, Y., & Prestwich, G. D. (2002). Cancer-targeted polymeric drugs. *Curr Cancer Drug Targets*, 2(3), 209–226.
- Majoros, I. J., Myc, A., Thomas, T., Mehta, C. B., & Baker, J. R., Jr. (2006). PAMAM dendrimer-based multifunctional conjugate for cancer therapy: Synthesis, characterization, and functionality. *Biomacromolecules*, 7(2), 572–579.
- Malik, N., Evagorou, E. G., & Duncan, R. (2000). Dendrimers: Relationship between structure and biocompatibility in vitro, and preliminary studies on the biodistribution of <sup>125</sup>I-labelled polyamidoamine dendrimers in vivo. *J Control Release*, 65(1–2), 133–148.
- Malik, N., Evagorou, E. G., & Duncan, R. (1999). Dendrimer-platinate: A novel approach to cancer chemotherapy. *Anticancer Drugs*, 10(8), 767–776.

- Maraval, V., Pyzowski, J., Caminade, A. M., & Majoral, J. P. (2003). "Lego" chemistry for the straightforward synthesis of dendrimers. *J Org Chem*, *68*, 6043–6046.
- Mecke, A., Majoros, I. J., Patri, A. K., Baker, J. R., Jr., Holl, M. M., & Orr, B. G. (2005). Lipid bilayer disruption by polycationic polymers: The roles of size and chemical functional group. *Langmuir*, *21*(23), 10348–10354.
- Mecke, A., Uppuluri, S., Sassanella, T. M., Lee, D. K., Ramamoorthy, A., Baker, J. R., Jr., Orr, B. G., & Banaszak Holl, M. M. (2004). Direct observation of lipid bilayer disruption by poly (amidoamine) dendrimers. *Chem Phys Lipids*, *132*(1), 3–14.
- Milhem, O. M., Myles, C., McKeown, N. B., Attwood, D., & D'Emanuele, A. (2000). Polyamidoamine starburst dendrimers as solubility enhancers. *Int J Pharm*, *197*(1–2), 239–241.
- Namazi, H., & Adeli, M. (2005). Dendrimers of citric acid and poly (ethylene glycol) as the new drug-delivery agents. *Biomaterials*, *26*(10), 1175–1183.
- Padilla De Jesus, O. L., Ihre, H. R., Gagne, L., Frechet, J. M., & Szoka, F. C., Jr. (2002). Polyester dendritic systems for drug delivery applications: In vitro and in vivo evaluation. *Bioconjug Chem*, *13*(3), 453–461.
- Patri, A. K., Kukowska-Latallo, J. F., & Baker, J. R., Jr. (2005). Targeted drug delivery with dendrimers: Comparison of the release kinetics of covalently conjugated drug and non-covalent drug inclusion complex. *Adv Drug Deliv Rev*, *57*(15), 2203–2214.
- Potschke, D., Ballauff, M., Lindner, P., Fischer, M., & Vogtle, F. (1999). Analysis of the structure of dendrimers in solution by small-angle neutron scattering including contrast variation. *Macromolecules*, *32*(12), 4079–4087.
- Prosa, T. J., Bauer, B. J., & Amis, E. J. (2001). From stars to spheres: A SAXS analysis of dilute dendrimer solutions. *Macromolecules*, *34*(14), 4897–4906.
- Quintana, A., Raczka, E., Piehler, L., Lee, I., Myc, A., Majoros, I., Patri, A. K., Thomas, T., Mule, J., & Baker, J. R., Jr. (2002). Design and function of a dendrimer-based therapeutic nanodevice targeted to tumor cells through the folate receptor. *Pharm Res*, *19*(9), 1310–1316.
- Rajca, A. (1991). Synthesis of 1,3-connected polyarylmethanes. *J Org Chem*, *56*(7), 2557–2563.
- Rathgeber, S., Pakula, T., & Urban, V. (2004). Structure of star-burst dendrimers: A comparison between small angle x-ray scattering and computer simulation results. *J Chem Phys*, *121*(8), 3840–3853.
- Roberts, J. C., Bhalgat, M. K., & Zera, R. T. (1996). Preliminary biological evaluation of polyamidoamine (PAMAM) Starburst dendrimers. *J Biomed Mater Res*, *30*(1), 53–65.
- Rosenfeldt, S., Karpuk, E., Lehmann, M., Meier, H., Lindner, P., Harnau, L., & Ballauff, M. (2006). The solution structure of stilbenoid dendrimers: A small-angle scattering study. *Chemphyschem*, *7*(10), 2097–2104.
- Sadler, K., & Tam, J.P. (2002). Peptide dendrimers: Applications and synthesis. *J Biotechnol*, *90*(3–4), 195–229.
- Sakamoto, Y., Suzuki, T., Miura, A., Fujikawa, H., Tokito, S., & Taga, Y. (2000). Synthesis, characterization, and electron-transport property of perfluorinated phenylene dendrimers. *J Am Chem Soc*, *122*(8), 1832–1833.
- Sakthivel, T., Toth, I., & Florence, A. T. (1999). Distribution of a lipidic 2.5 nm diameter dendrimer carrier after oral administration. *Int J Pharm*, *183*(1), 51–55.
- Sanchez-Sancho, F., Perez-Inestrosa, E., Suau, R., Mayorga, C., Torres, M. J., & Blanca, M. (2002). Dendrimers as carrier protein mimetics for Ige antibody recognition. Synthesis and characterization of densely penicilloylated dendrimers. *Bioconjug Chem*, *13*(3), 647–653.

- Sedlakova, P., Svobodova, J., Miksik, I., & Tomas, H. (2006). Separation of poly(amidoamine) (PAMAM) dendrimer generations by dynamic coating capillary electrophoresis. *J Chromatogr B Analyt Technol Biomed Life Sci*, 841(1–2), 135–139.
- Shaunak, S., Thomas, S., Gianasi, E., Godwin, A., Jones, E., Teo, I., Mireskandari, K., Luthert, P., Duncan, R., Patterson, S., Khaw, P., & Brocchini, S. (2004). Polyvalent dendrimer glucosamine conjugates prevent scar tissue formation. *Nat Biotechnol*, 22(8), 977–984.
- Shi, X., Patri, A. K., Lesniak, W., Islam, M. T., Zhang, C., Baker, J. R., Jr., & Balogh, L. P. (2005). Analysis of poly(amidoamine)-succinamic acid dendrimers by slab-gel electrophoresis and capillary zone electrophoresis. *Electrophoresis*, 26(15), 2960–2967.
- Singh, B., & Florence, A. T. (2005). Hydrophobic dendrimer-derived nanoparticles. *Int J Pharm*, 298(2), 348–353.
- Svenson, S., & Tomalia, D. A. (2005). Dendrimers in biomedical applications – reflections on the field. *Adv Drug Deliv Rev*, 57(15), 2106–2129.
- Tack, F., Bakker, A., Maes, S., Dekeyser, N., Bruining, M., Elissen-Roman, C., Janicot, M., Brewster, M., Janssen, H. M., de Waal, B. F., Franssen, P. M., Lou, X., & Meijer, E. W. (2006). Modified poly(propylene imine) dendrimers as effective transfection agents for catalytic DNA enzymes (DNAzymes). *J Drug Target*, 14(2), 69–86.
- Tajarobi, F., El-Sayed, M., Rege, B. D., Polli, J. E., & Ghandehari, H. (2001). Transport of poly amidoamine dendrimers across Madin-Darby canine kidney cells. *Int J Pharm*, 215(1–2), 263–267.
- Takakura, Y., Mahato, R. I., & Hashida, M. (1998). Extravasation of macromolecules. *Adv Drug Deliv Rev*, 34(1), 93–108.
- Tang, M. X., Redemann, C. T., & Szoka, F. C., Jr. (1996). In vitro gene delivery by degraded polyamidoamine dendrimers. *Bioconjug Chem*, 7(6), 703–714.
- Tang, S., Martinez, L. J., Sharma, A., & Chai, M. (2006). Synthesis and characterization of water-soluble and photostable L-DOPA dendrimers. *Org Lett*, 8, 4421–4424.
- Tansey, W., Ke, S., Cao, X. Y., Pasuelo, M. J., Wallace, S., & Li, C. (2004). Synthesis and characterization of branched poly(L-glutamic acid) as a biodegradable drug carrier. *J Control Release*, 94(1), 39–51.
- Tomalia, D. A. (1993). Starburst<sup>TM</sup>/cascade dendrimers: Fundamental building blocks for new nanoscopic chemistry set. *Aldrichimica Acta*, 26(4), 91–101.
- Tomalia, D. A. (2004). Birth of a new macromolecular architecture: Dendrimers as quantized building blocks for nanoscale synthetic organic chemistry. *Aldrichimica Acta*, 37(2), 39–57.
- Tomalia, D. A., Naylor, A. M., & Goddard III, W. A. (1990). Starburst dendrimers. Molecular-level control of size, shape, surface chemistry, topology, and flexibility from atoms to macroscopic matter. *Angew Chem Int Ed Engl*, 29(2), 138–175.
- Tomlinson, R., Heller, J., Brocchini, S., & Duncan, R. (2003). Polyacetal-doxorubicin conjugates designed for pH-dependent degradation. *Bioconjug Chem*, 14(6), 1096–1106.
- Torchilin, V. P. (2006). Multifunctional nanocarriers. *Adv Drug Deliv Rev*, 58(14), 1532–1555.
- Trehwella, J., Gallagher, S. C., Krueger, J. K., & Zhao, J. (1998). Neutron and x-ray solution scattering provide insights into biomolecular structure and function. *Sci Prog*, 81(Pt 2), 101–122.
- Turnbull, W. B., & Stoddart, J. F. (2002). Design and synthesis of glycodendrimers. *J Biotechnol*, 90(3–4), 231–255.

- Velazquez, A. J., Carnahan, M. A., Kristinsson, J., Stinnett, S., Grinstaff, M. W., & Kim, T. (2004). New dendritic adhesives for sutureless ophthalmic surgical procedures: In vitro studies of corneal laceration repair. *Arch Ophthalmol*, 122(6), 867–870.
- Wang, S. J., Brechbiel, M., & Wiener, E. C. (2003). Characteristics of a new MRI contrast agent prepared from polypropyleneimine dendrimers, generation 2. *Invest Radiol*, 38(10), 662–668.
- Wiener, E. C., Brechbiel, M. W., Brothers, H., Magin, R. L., Gansow, O. A., Tomalia, D. A., & Laterbur, P. C. (1994). Dendrimer-based metal chelates: A new class of magnetic resonance imaging contrast agents. *Magn Reson Med*, 31(1), 1–8.
- Wignall, G. D., & Melnichenko, Y. B. (2005). Recent applications of small-angle neutron scattering in strongly interacting soft condensed matter. *Rep Prog Phys*, 68(8), 1761–1810.
- Wiwattanapatapee, R., Carreno-Gomez, B., Malik, N., & Duncan, R. (2000). Anionic PAMAM dendrimers rapidly cross adult rat intestine in vitro: A potential oral delivery system? *Pharm Res*, 17(8), 991–998.
- Wu, P., Malkoch, M., Hunt, J. N., Vestberg, R., Kaltgrad, E., Finn, M. G., Fokin, V. V., Sharpless, K. B., & Hawker, C. J. (2005). Multivalent, bifunctional dendrimers prepared by click chemistry. *Chem Commun (Camb)* (46), 5775–5777.
- Wu, P., Feldman, A. K., Nugent, A. K., Hawker, C. J., Scheel, A., Voit, B., Pyun, J., Frechet, J. M., Sharpless, K. B., & Fokin, V. V. (2004a). Efficiency and fidelity in a click-chemistry route to triazole dendrimers by the copper(I)-catalyzed ligation of azides and alkynes. *Angew Chem Int Ed Engl*, 43(30), 3928–3932.
- Wu, X. Y., Huang, S. W., Zhang, J. T., & Zhuo, R. X. (2004b). Preparation and characterization of novel physically cross-linked hydrogels composed of poly(vinyl alcohol) and amine-terminated polyamidoamine dendrimer. *Macromol Biosci*, 4(2), 71–75.
- Yoo, H., & Juliano, R. L. (2000). Enhanced delivery of antisense oligonucleotides with fluorophore-conjugated PAMAM dendrimers. *Nucleic Acids Res*, 28(21), 4225–4231.
- Yordanov, A. T., Lodder, A. L., Woller, E. K., Cloninger, M. J., Patronas, N., Milenic, D., & Brechbiel, M. W. (2002). Novel iodinated dendritic nanoparticles for computed tomography (CT) imaging. *Nano Lett*, 2(6), 595–599.
- Zhuo, R. X., Du, B., & Lu, Z. R. (1999). In vitro release of 5-fluorouracil with cyclic core dendritic polymer. *J Control Release*, 57(3), 249–257.
- Ziemer, L. S., Lee, W. M., Vinogradov, S. A., Sehgal, C., & Wilson, D. F. (2005). Oxygen distribution in murine tumors: Characterization using oxygen-dependent quenching of phosphorescence. *J Appl Physiol*, 98(4), 1503–1510.